LA-6518-MS
Informal Report

ENDF-244
INDC(USA)-76/U
NEANDC(US)-200/U
ERDA/NDC-6/U

MASTER

UC-34c and UC-79
Reporting Date: September 1976
Issued: October 1976

Light Element Standard Cross Sections for ENDF/B Version IV

by

G. M. Hale
L. Stewart
P. G. Young

los alamos
scientific laboratory
of the University of California
LOS ALAMOS, NEW MEXICO 87545

UNITED STATES
ENERGY RESEARCH AND DEVELOPMENT ADMINISTRATION
CONTRACT W-7405-ENG. 36

This work was supported by US Energy Research and Development Administration, Division of Reactor Development and Demonstration.

Printed in the United States of America. Available from
National Technical Information Service
U.S. Department of Commerce
5285 Port Royal Road
Springfield, VA 22161
Price: Printed Copy $4.00 Microfiche $2.25

LIGHT ELEMENT STANDARD CROSS SECTIONS FOR ENDF/B VERSION IV

by

G. M. Hale, L. Stewart, and P. G. Young

ABSTRACT

Several light-element standard cross-section evaluations in the ENDF/B-IV file are described and compared with experimental measurements. The hydrogen scattering cross section has long been accepted as a standard since it is essentially equal to the total cross section which is well known and varies smoothly with incident neutron energy. The $^{3}He(n,p)T$, $^{6}Li(n,t)\alpha$, $^{10}B(n,\alpha_0)^{7}Li$, and $^{10}B(n,\alpha_1)^{7}Li^{*}$(478-keV γ) reactions have positive Q values and large thermal cross sections which make them ideal to use in neutron flux monitors. The Yale phase shifts were used to generate the hydrogen elastic scattering cross section and angular distributions while comprehensive R-matrix analyses were performed to determine the ^{6}Li and ^{10}B cross sections.

I. INTRODUCTION

This report describes several of the light element standard cross-section evaluations that are included in Version IV of ENDF/B.[1] It is limited to those reactions for which the Los Alamos Scientific Laboratory has the primary responsibility and is intended as a supplement to an earlier but less detailed report by Magurno[2] which includes all of the Version IV standards.

The main criteria for the choice of a standard cross section are that it be a smooth function of energy and well determined experimentally; in addition, the response function of the detector in which the cross section is employed assumes great importance. While positive Q reactions enhance detector response functions, they also produce very large low-energy backgrounds. Therefore, neutron sources and geometry must be chosen with great care.

Elastic neutron scattering from hydrogen, for which the cross section is essentially equal to the total cross section above a few eV, is the only reaction which satisfies the criterion of smoothness over the entire energy range to 20 MeV. Unfortunately, however, the hydrogen recoil does not have enough energy to produce a useful response* at low-incident neutron energies in most detector configurations, and positive Q reactions must be employed in flux monitors below a few keV. The light-element standard evaluations for ENDF/B-IV described in this report are listed in Table I along with a few of their important properties.

TABLE I

Reaction	Mat#	Standard	Q-Value (MeV)	Recommended Energy Range
$^{1}H(n,n)^{1}H$	1269	$\sigma_{elas}(E_n)$ $\sigma_{elas}(E_n,\theta_n)$	0	1 keV-20 MeV
$^{3}He(n,p)T$	1146	$\sigma_{n,p}(E_n)$	+ 0.7645	thr. - 1 MeV
$^{6}Li(n,t)^{4}He$	1271	$\sigma_{n,t}(E_n)$	+ 4.786	thr. - 100 keV
$^{10}B(n,\alpha)^{7}Li$	1273	$\sigma_{n,\alpha}(E_n)$	+ 2.790	thr. - 100 keV
$^{10}B(n,\alpha_1\gamma)^{7}Li$	1273	$\sigma_{n,\alpha_1\gamma}(E_n)$	+ 2.312	thr. - 100 keV

II. $^{1}H(n,n)^{1}H$ ELASTIC SCATTERING CROSS SECTION AND ANGULAR DISTRIBUTION

The elastic and total cross sections for hydrogen are essentially equal above a few eV, and the total cross section is the best known and most often recommended of the standard cross sections. It satisfies the most important requirements for standards in that $\sigma(E_n)$ shows no structure up to 20 MeV, the cross section is well known, the scattering is isotropic in the center-of-mass system (±4%) up to 20 MeV, and hydrogen is relatively easy to incorporate into various counter types.

*The 2.2-MeV γ from the $^{1}H(n,\gamma)D$ reaction is sometimes used in a flux monitor instead of the recoil proton thereby taking advantage of a positive Q reaction to employ a hydrogen counter at low energies. A discussion of this reaction, however, is not included in this report.

The extensive theoretical analysis of fast-neutron measurements by Hopkins and Breit[3] was used to generate the scattering cross section and angular distributions of the neutrons for the ENDF/B-IV file.[4] The code and the Yale phase shifts[5] were obtained from Hopkins[6] in order to obtain the data on a fine-energy grid. Pointwise angular distributions were produced to improve the precision over that obtained from the published Legendre coefficients.* The phase shifts were also used to extend the energy range down below 200 keV as represented in the original paper.[3]

At 100 eV, the elastic cross section calculated from the phase shifts is 20.449 barns, in excellent agreement with the thermal value of 20.442 derived by Davis and Barschall.[7] Therefore, for the ENDF/B-IV evaluation, the free-atom scattering cross section is assumed to be constant below 100 eV and equal to the value calculated from the Yale phase shifts at 100 eV giving a thermal cross section of 20.449 b.

Total cross-section measurements are compared with the evaluation in Fig. 1 for the energy range from 10 eV to 0.5 MeV. Similarly, Figs. 2 and 3 compare the evaluation with measured data from 0.5 to 20 MeV. The agreement with the earlier experiments shown in Fig. 2 is quite good over the entire energy range. The 1969 data of Schwartz[42] included in Fig. 3, however, lie slightly below the evaluation over most of the energy range even though agreement with the 1972 results of Clement[43] is quite acceptable.

Unfortunately, few <u>absolute</u> values of the angular dependence of the neutrons (or recoil protons) exist and even the relative measurements are often restricted to less than half of the angular range. The experiment of Oda[24] at 3.1 MeV is not atypical of the earlier distributions which, as shown in Fig. 4, does not agree with the phase-shift predictions. Near 14 MeV, the T(d,n) neutron source has been employed in many experiments to determine the angular distributions. A composite of these measurements is compared with ENDF/B-IV in Fig. 5A. Note that most of the experiments are in reasonable agreement on a relative scale, but 10% discrepancies frequently appear among the data sets. The measurements of Cambou[50] average more than 5% lower than the predicted curve and differences of 5% or more are occasionally apparent among the data of a single set. Figure 5B

*For E_n = 30 MeV, the difference in the 180° cross section is ~ 1% as calculated from the Legendre coefficients[3] compared to that calculated from the phase shifts.

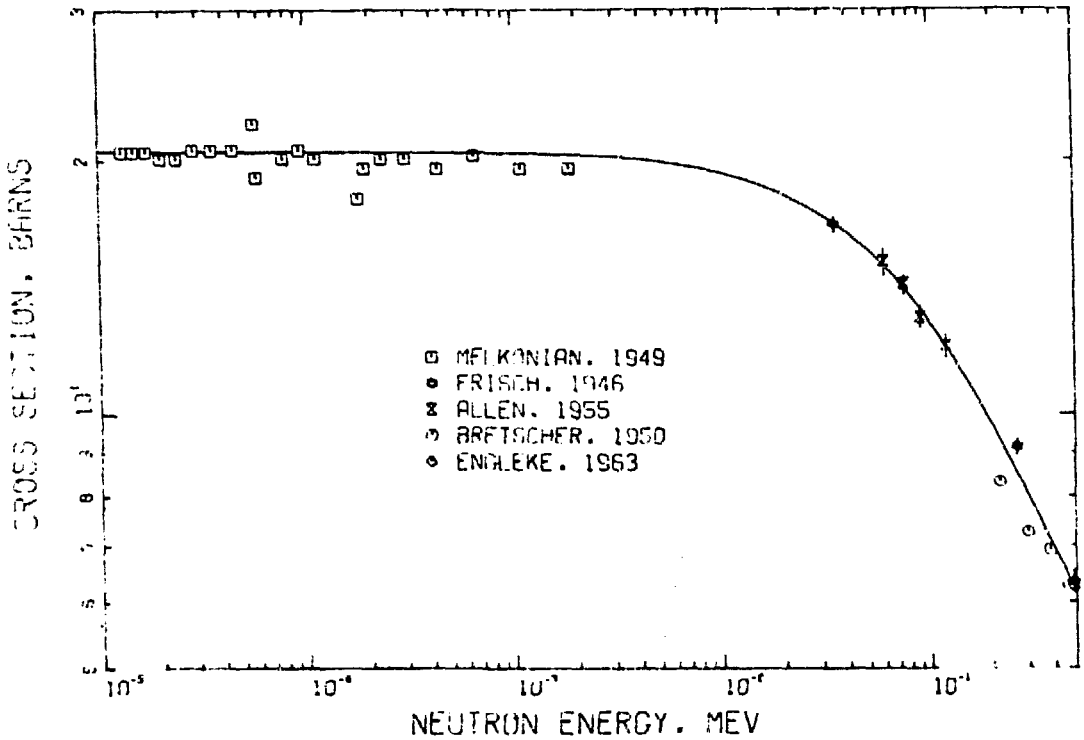

Fig. 1.
Total cross section for hydrogen from 1 x 10^{-5} eV to 500 keV. The ENDF/B-IV evaluation is compared to the measurements of Refs. 8-12.

shows the measurements of Galonsky[51] at 17.9 MeV compared with the evaluation. Again, the agreement on an absolute basis is quite poor.

Elastic scattering angular distributions at 0.1, 5, 10, 20, and 30 MeV are provided in Ref. 1 as Legendre expansion coefficients. Using the Hopkins-Breit phase-shift program and the Yale phase shifts, additional and intermediate energy points were calculated for the Version IV evaluation.[4] As shown in Figs. 5-16 of Ref. 4, the angular distributions are neither isotropic below 10 MeV nor symmetric about 90° above 10 MeV as assumed in earlier evaluations. In this evaluation, the angular distribution at 100 keV is assumed to be isotropic since the calculated 180°/0° ratio is very nearly unity, that is, 1.0011. At 500 keV, this ratio approaches 1.005. Therefore, the pointwise normalized probabilities as a function of the center-of-mass scattering angle are provided at the following energies: 10^{-5} eV (isotropic), 100 keV (isotropic), 500 keV, and at 1-MeV intervals from 1 to 20 MeV.

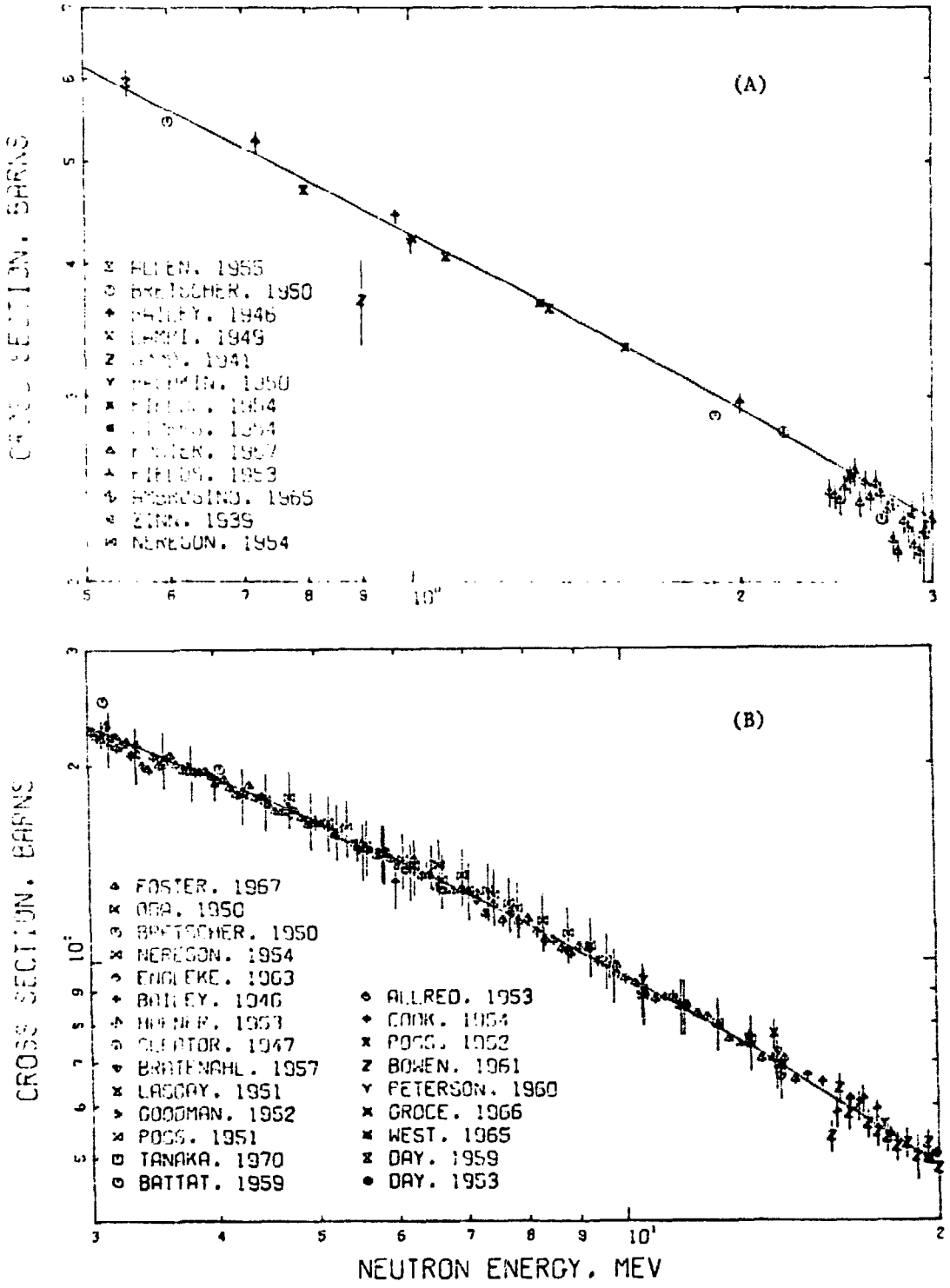

Fig. 2.
Total cross section for hydrogen from 500 keV to 20 MeV. The ENDF/B-IV evaluation is compared to measurements reported in Refs. 10-41.

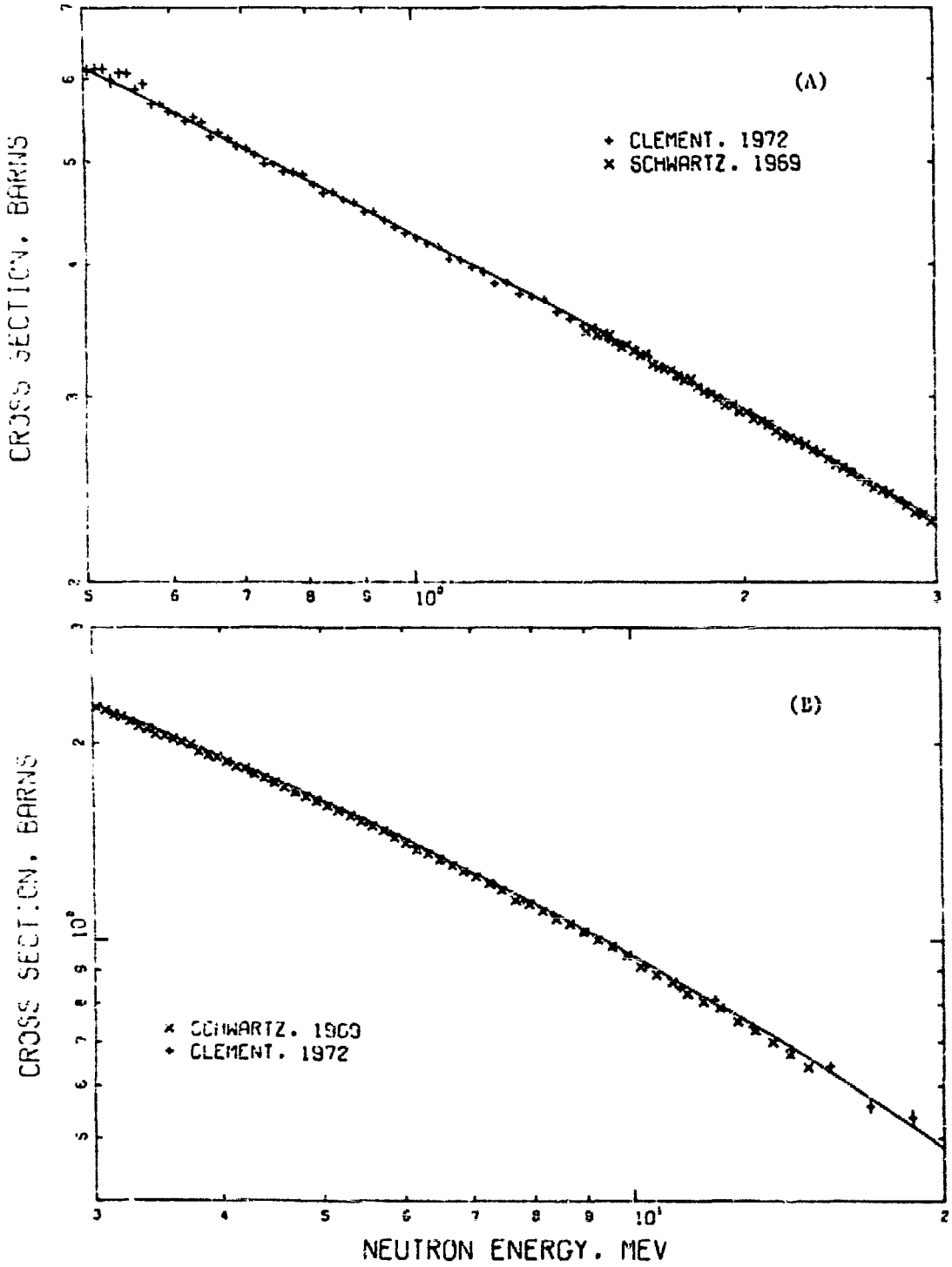

Fig. 3.
Total cross section for hydrogen from 500 keV to 20 MeV. The ENDF/B-IV evaluation is compared to measurements reported in Refs. 42 and 43.

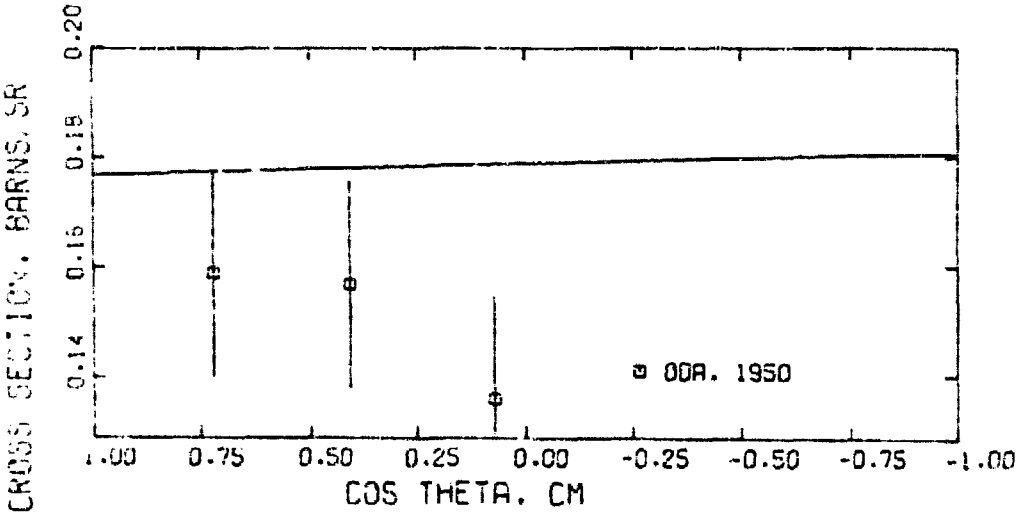

Fig. 4.
Angular distribution of the neutrons elastically scattered from hydrogen at 3.1 MeV. ENDF/B-IV is compared with the experimental values of Oda.[24]

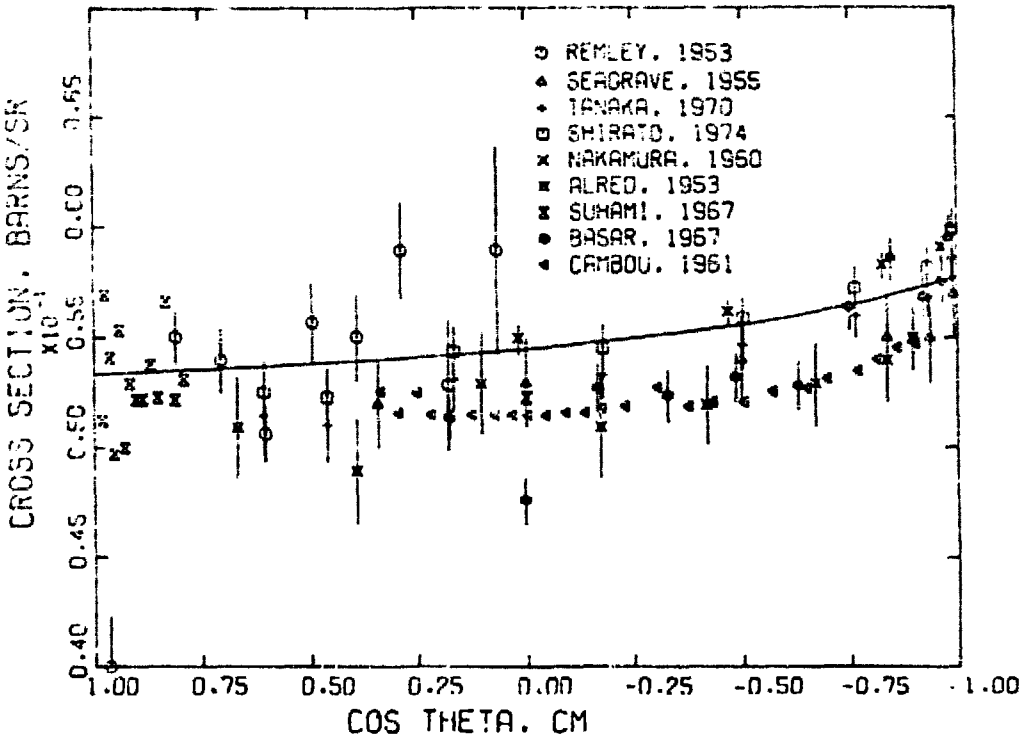

Fig. 5A.
Angular distribution of the neutrons elastically scattered from hydrogen at energies near 14 MeV. The experimental data shown were reported in Refs. 31, 33 and 44-50.

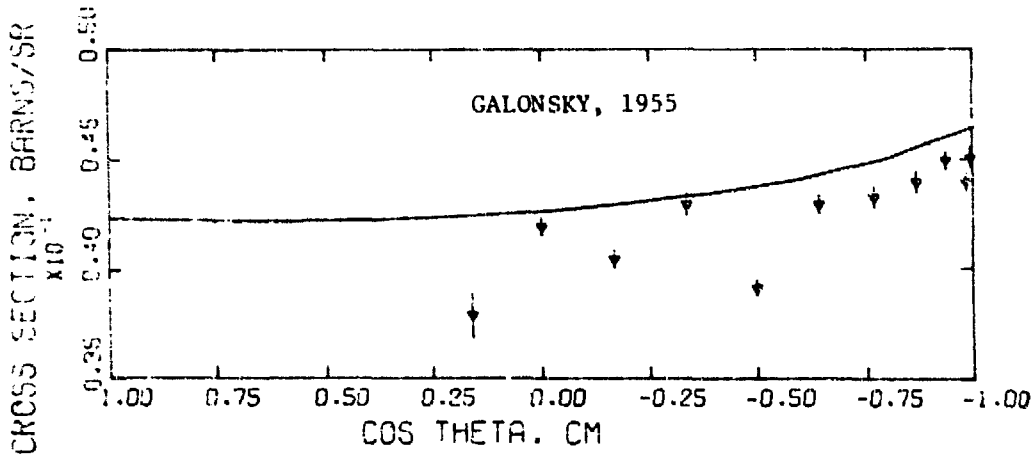

Fig. 5B.
Angular distribution of the neutrons elastically scattered from hydrogen at energies near 17.8 MeV. The experimental data shown were reported in Ref. 51.

Certainly the Hopkins-Breit phase shifts reproduce reasonably well the measured angular distributions near 14 MeV. It is important, however, that experiments be made at two or three energies which would, hopefully, further corroborate this analysis. Near 14 MeV, the energy-dependent total cross section is presently assumed to be known to ~ 1% and the angular distribution to ~ 2-3%. At lower energies where the angular distributions approach isotropy, the error estimate on the angular distribution is less than 1%.

It should be pointed out that errors involved in using hydrogen as a standard depend upon the experimental techniques employed and therefore may be significantly larger than the errors placed on the standard cross section. The elastic angular distribution measurements of neutrons scattered by hydrogen, which are available today, seem to indicate that $\sigma(\Theta)$ is difficult to measure with the precision ascribed to the reference standard. If this is the case, then the magnitude of the errors in the $\sigma(\Theta)$ measurements might be indicative of error assignments which should be made on hydrogen flux monitors. That is, it is difficult to assume that hydrogen scattering can be implemented as a standard

with much higher precision than it can be measured. Even though better agreement with many past measurements can be reached by renormalizing the absolute scales, such action may not always be warranted.

At this time, no attempt has been made to estimate the effect of errors on the energy scale in ENDF/B. It is clear, however, that a small energy shift would produce a large change in the cross section, especially at low energies. For example, a 50-keV shift in energy near 1 MeV would produce a change in the standard cross section of approximately 2½%. Therefore, precise determination of the incident neutron energy and the energy spread could be very important in employing hydrogen as a cross-section standard, depending upon the experimental technique.

III. ^{3}He(n,p)T CROSS SECTION

The ENDF/B-IV evaluation was performed in 1968 and accepted by the CSEWG Standards Subcommittee for the ENDF/B-III file[52] in 1971. No changes have been recommended for this file; therefore ENDF/B-IV was carried over from ENDF/B-III. This standard is recommended for use up to approximately 1 MeV.

The thermal cross section of 5327 b was derived from precise measurements by Als-Nielsen and Dietrich[53] of the total cross section up to an energy of 11 eV. No experimental measurements on the ^{3}He(n,p) reaction are available below ~ 5 keV, and the cross section was assumed to follow 1/v up to 1.7 keV. The evaluation is compared with the available data below 10 keV in Fig. 6. For convenience, the inset includes tabular values of the elastic, (n,p) and total cross sections at a few energies up to 1 keV.

Up to 10 keV, the evaluation is a reasonable representation of the 1966 results of Gibbons and Macklin[54] and an average of their cross sections measured in 1963.[55] These experiments, which extend to 100 keV, are compared with ENDF/B-IV in Fig. 7.

From 100 keV to 1 MeV, additional experiments are available. The evaluation is heavily weighted by the data of Refs. 54 and 55 and the cross sections of Perry et al.[56] as given in Fig. 8. Note that these three measurements are in good agreement among themselves but are higher than the measurements of Batchelor et al.[57] and of Sayres et al.[58] On the other hand, Sayres et al. measure an elastic cross section much higher than reported by Seagrave et al.[59] (noted on the same figure).

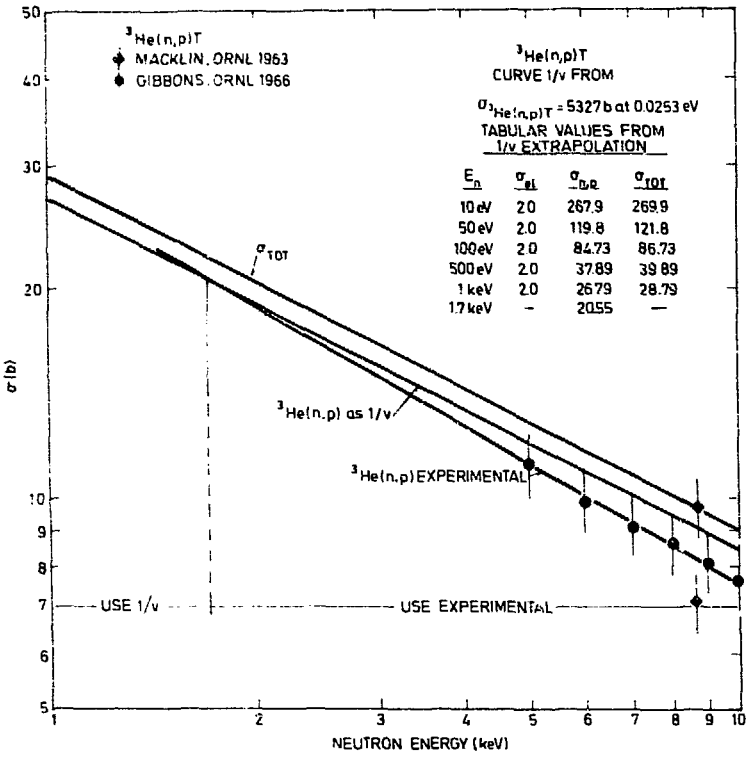

Fig. 6.
The (n,p) and total cross sections for ^{3}He from 1 to 10 keV. The curve drawn through the experimental points deviates from 1/v at 1.7 keV.

In 1970, Costello et al.[60] measured the (n,p) cross section from 300 keV to 1 MeV and obtained essentially a constant value of 900 mb over this energy range. Agreement of the Costello data with this evaluation above 500 keV is excellent, although from 300 to 400 keV, their measurements are more than 10% lower than ENDF/B-IV.

Finally, Lopez et al.[61] measured the relative ratio of the counting rates between ^{3}He and BF_3 proportional counters from 218 eV to 521 keV. To provide a comparison between these two standard cross sections, the Lopez ratios were normalized at 218 eV to the Version IV ratios. Then, by using this evaluation for the ^{3}He(n,p) cross section to convert the Lopez ratio measurements to ^{10}B cross sections, reasonable agreement with Version IV ^{10}B(n,α) is obtained.

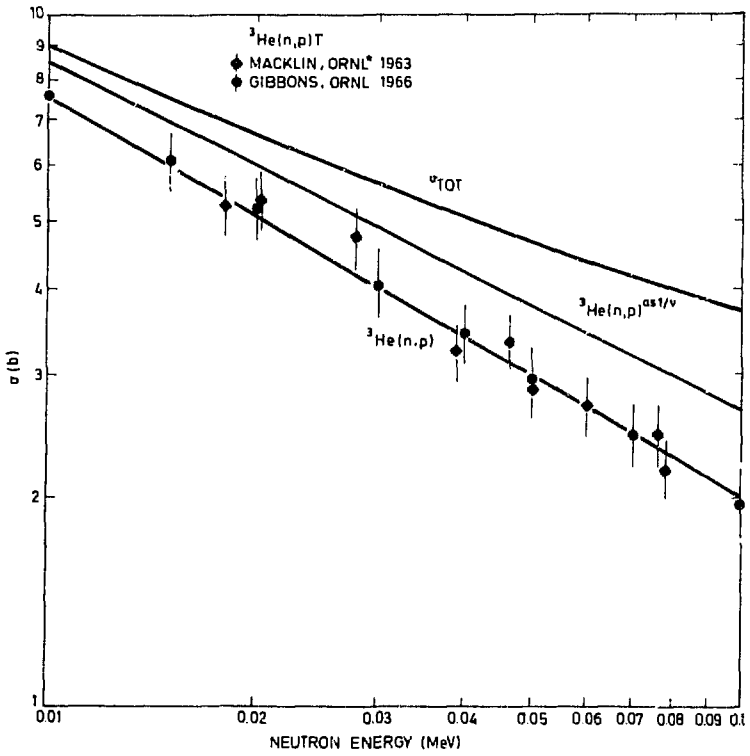

Fig. 7.
The (n,p) and total cross sections for ^{3}He from 10 to 100 keV.

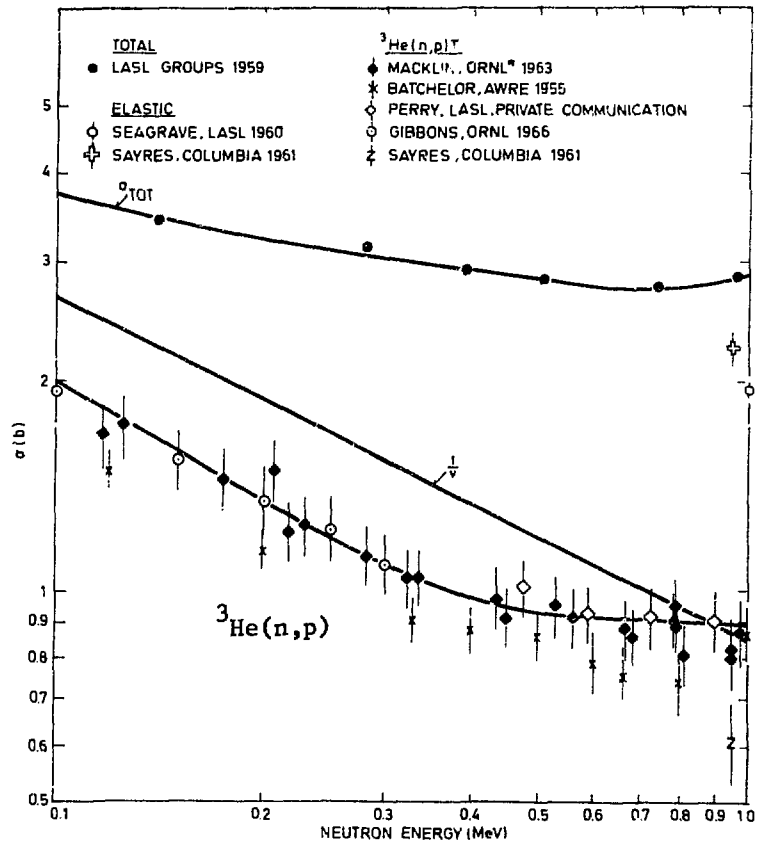

Fig. 8.
The (n,p), elastic, and total cross sections for ^{3}He from 100 keV to 1 MeV. The Costello data[60] have been omitted for the sake of clarity.

It should be noted, however, that the energy points are too sparse above a few keV to reproduce the structure observed in ^{10}B.

Although the thermal (n,p) cross section is known to better than 1%, the energy at which this cross section deviates from 1/v is not well established. It should also be emphasized that experiments have not been carried out from 11 eV to a few keV, thereby placing severe restrictions upon the accuracy accompanying the use of the $^{3}He(n,p)T$ cross-section standard. The 10% error estimates on the ORNL experimental data are directly related to the uncertainties in the analysis of the target samples employed. Certainly, further absolute measurements are needed on this cross-section standard, especially above ~ 100 eV.

IV. $^{6}Li(n,\alpha)t$ CROSS SECTION

In the region below E_n = 1.7 MeV, the $^{6}Li(n,\alpha)$ cross-section evaluation is based on a comprehensive R-matrix analysis of reactions in the ^{7}Li system. The R-matrix formalism[62] is well suited for describing reactions in this system, since it accounts for both the 1/v behavior and resonance structure of the cross sections. Furthermore, the cross sections from such an analysis satisfy general physical constraints imposed by unitarity, causality, and conservation of total angular momentum and parity.

Data from the reactions $^{6}Li(n,n)^{6}Li$, $^{6}Li(n,\alpha)T$, and $^{4}He(t,t)^{4}He$ at energies corresponding to E_n below 1.7 MeV, were fitted simultaneously using the multichannel, multilevel R-matrix analysis code, EDA.[63] Starting from the usual parameters of the R matrix, eigenvalues ϵ_λ, reduced width amplitudes $\gamma_{\lambda c}$, and channel radii a_c, the code calculates unitary collision-matrix elements in accordance with general relations given by Lane and Thomas,[64] then forms experimental observables for each reaction using the M-matrix trace formalism of Wolfenstein.[65] An automated search algorithm adjusts the resonance parameters to achieve a "best fit" to all the data included in the analysis in a least-squares sense. Quantities specifying the two-body channels of the ^{7}Li system considered in this analysis are given in Table II.

The types of data considered for each reaction, along with references for the measurements included in the analysis, are listed in Table III. Starting values for the resonance parameters were chosen to accomodate all the known levels[87] in ^{7}Li below 10-MeV excitation energy, as well as distant-level contributions in each state. The fits obtained from searching over the resonance parameters are described briefly for each reaction below.

TABLE II

CHANNEL QUANTITIES FOR THE ^{7}Li SYSTEM ANALYSIS

Channel	Channel Radius (f)	Channel Spin (s)	ℓ_{max}
n-^{6}Li	4.20	1/2, 3/2	1
t-α	4.02	1/2	4

TABLE III

DATA INCLUDED IN THE ^{7}Li SYSTEM ANALYSIS

Reaction	Data Type	References
^{6}Li(n,n)^{6}Li	σ_{int}	66, 67
	$\sigma(\theta)$	66, 67, 68, 69
	$P(\theta)$	69
^{6}Li(n,t)^{4}He	σ_{int}	70, 71, 72
	$\sigma(\theta)$	73
n-^{6}Li	σ_T	74, 75
^{4}He(t,t)^{4}He	$\sigma(\theta)$ (E_t = 1.7-11 MeV)	76, 77
	$P(\theta)$	78

A. ^{6}Li(n,n)^{6}Li

Calculated values of the elastic integrated cross section are shown in Fig. 9 and compared with the experimental data of Lane[66] and Knitter[67] in Fig. 9B. The $5/2^-$ resonance at E_n = 250 keV, which dominates reactions in the ^{7}Li system in the keV range, is clearly evident in this cross section. Below the peak of the resonance, the R-matrix fit lies well above Lane's points, and agrees at low energies with measurements by Asami,[80] although these data were not included in the analysis. The shapes of the elastic angular distributions and polarizations are reproduced well by the calculations over the entire energy range.

B. ^{6}Li(n,t)^{4}He

The calculated value of the integrated cross section at thermal is 940 b., in exact agreement with the value obtained by Diment.[74] The 1/v dependence of

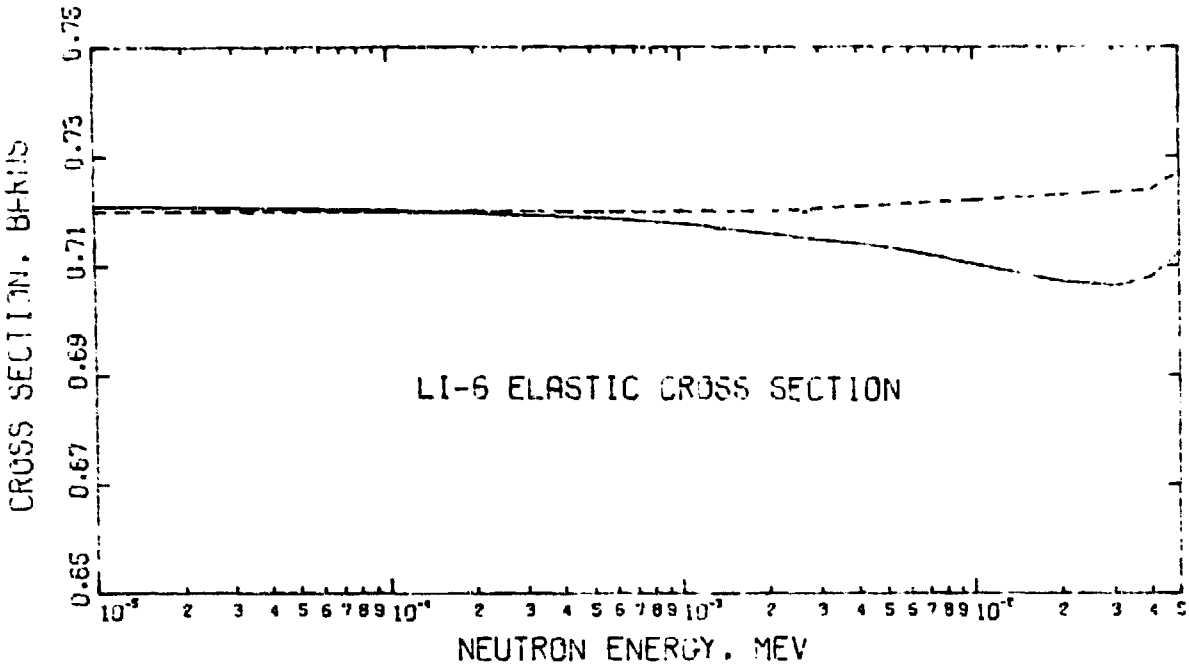

Fig. 9A.
$^{6}Li(n,n)^{6}Li$ integrated cross section for E_n between 10 eV and 50 keV. On this and all subsequent figures, the solid curve is ENDF/B-IV and the dashed curve is ENDF/B-III.

the calculated cross section at low energies comes from apparently distant-level contributions in both s-wave states, with the J = 1/2 transition contributing approximately 3 times the cross section of the J = 3/2 transition. Calculated and experimental data for neutron energies between 10 eV and 2 MeV are compared in Figs. 10A and 10B [note that the ordinate in Fig. 10A is $\sigma(E_n)\sqrt{E_n}$]. The calculations in the 1/v region agree well with the (n,α) $^{6}Li/^{10}B$ ratio measurements of Sowerby,[70] converted to $^{6}Li(n,\alpha)$ cross sections using the Version IV $^{10}B(n,\alpha)$. The calculated cross sections also agree well with Coates'[71] measurements below 35 keV, then rises to become 8% higher in the minimum at ~ 100 keV, and 20% higher at the peak of the $5/2^-$ resonance at 240 keV, as shown in Fig. 10B. On the back side of the resonance, the calculations remain slightly higher than Coates' values, following the measurements of Poenitz[72] and Fort[81] above 400 keV.

Thus, the resonance is broader and taller in the calculated cross section than in the measurements of Coates, though not as broad and tall as recent measurements of Friesenhahn[82] indicate. These differences between the calculated cross sections and the measurements, which involve shape as well as normalization,

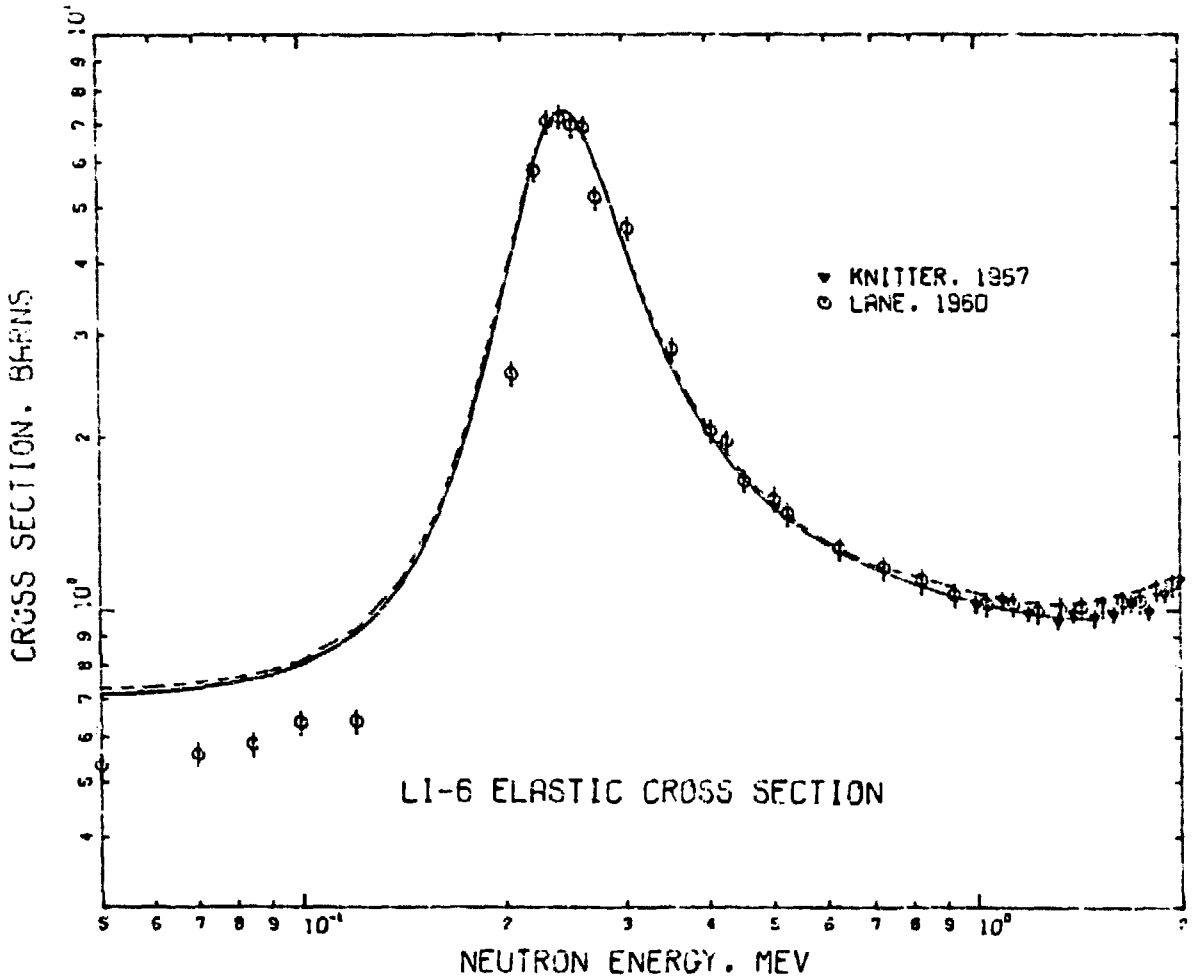

Fig. 9B.
$^6Li(n,n)^6Li$ integrated cross section for E_n between 50 keV and 2 MeV. The data are from Refs. 66 and 67.

appear to result from fitting simultaneously the precisely determined neutron total cross section described below.

C. $n-^6Li$, σ_T

The fit to the neutron total cross section from 10 eV to 2 MeV is shown in Fig. 11A and 11B. One sees that excellent agreement is obtained with measurements of Diment and Uttley.[74] This is partly due to the fact that these data were weighted heavily in the analysis by their small errors (typically ~ 1%). The energy of the resonance peak in the calculated total cross section is 247 keV, indicating that the experimentally observed ~ 7 keV shift relative to the

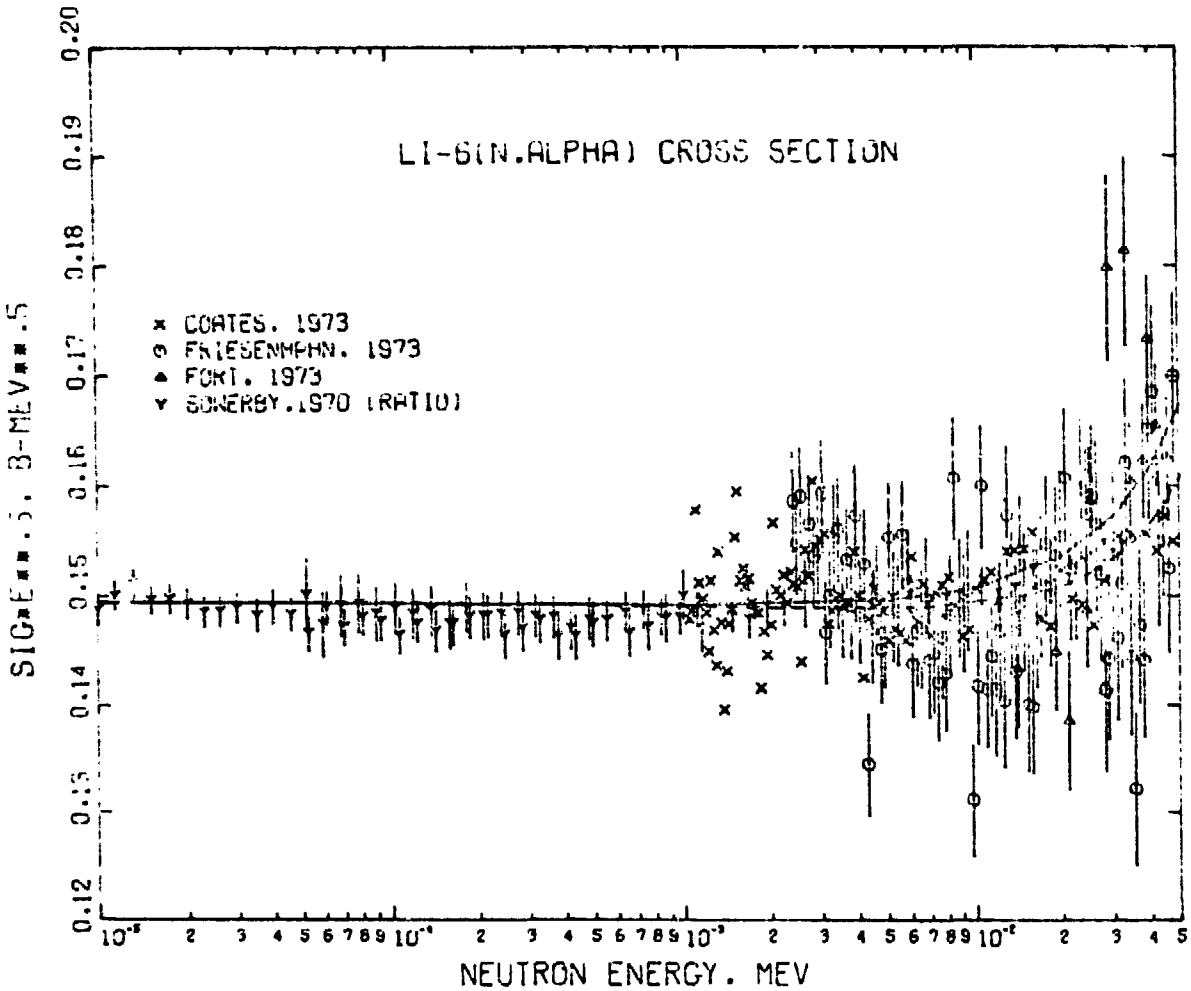

Fig. 10A.
The $^6Li(n,t)^4He$ integrated cross section for E_n in the range 10 eV to 50 keV. The data are from Refs. 70-71, and 81-82.

peak of the (n,t) cross section (240 keV) is real. In the calculations, this shift comes from interference of the resonant amplitude with the hard-sphere amplitude for elastic scattering, and with another $5/2^-$ level just below the neutron threshold.

D. $^4He(t,t)^4He$

Fits to a selection of differential cross-section and polarization measurements for $^4He(t,t)$ elastic scattering are shown in Fig. 12 to illustrate the consistency of the resonance parameters with the considerable structure evident in the data from this reaction. In particular, these data determine the parameters of most of the levels below the neutron threshold, and supply additional

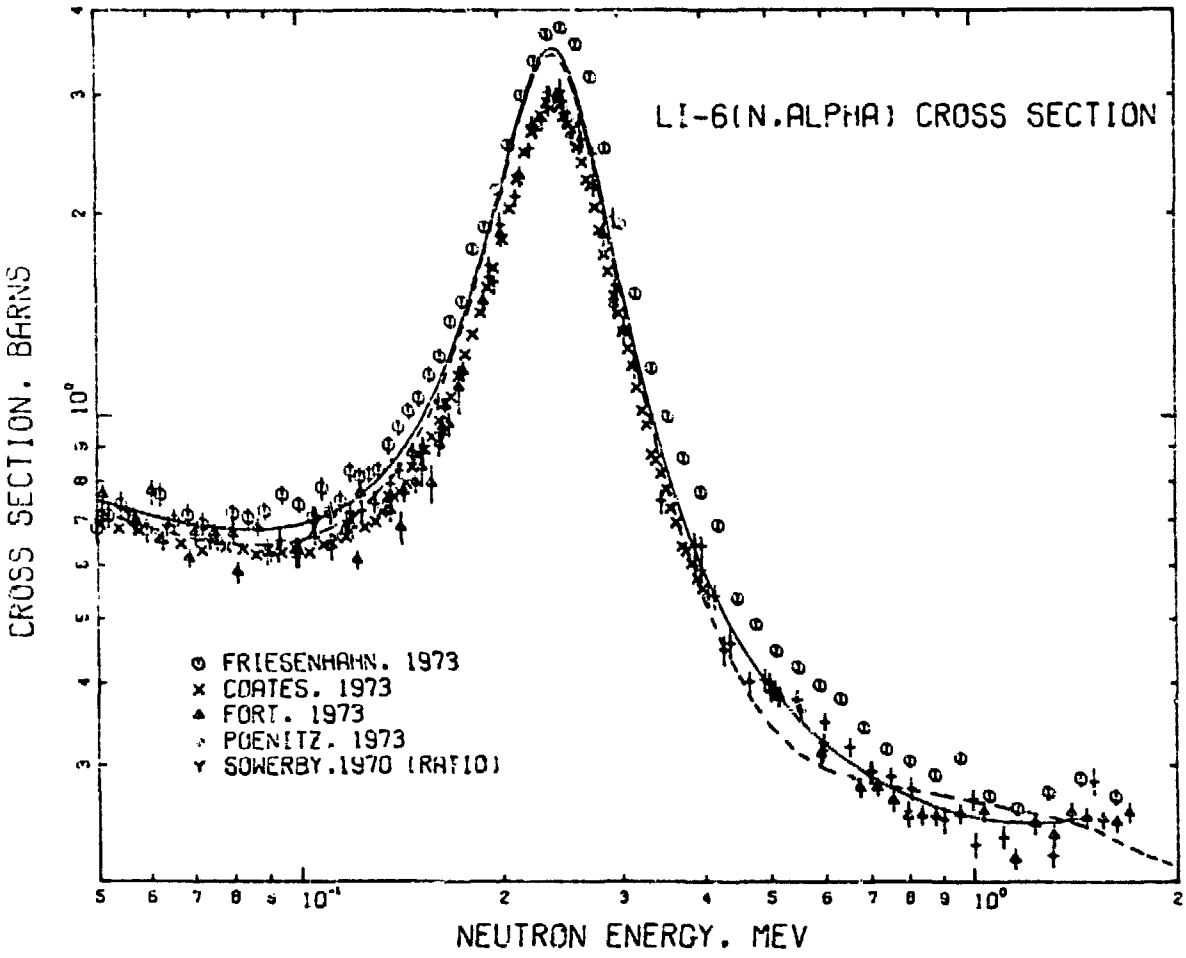

Fig. 10B.
The $^6Li(n,t)^4He$ integrated cross section for E_n in the range 50 keV to 2 MeV. The data are from Refs. 70-72, and 81-82.

constraints on the parameters of the important $5/2^-$ resonance at 250 keV. $^4He(t,t)$ measurements in the region of $5/2^-$ resonance available at the time this analysis was performed were not sufficiently accurate, however, to influence the fit nearly as much as did the neutron total cross section, for instance.

Although this analysis was completely independent of that used to provide the Version III evaluation for ^6Li at low energies, the results obtained are quite similar. This is because the results are highly constrained in both cases by fitting the accurate total cross-section measurements of Diment. Our analysis indicates that including the effects of all other known resonances and data from other reactions still does not sufficiently relax the single-level nature of the

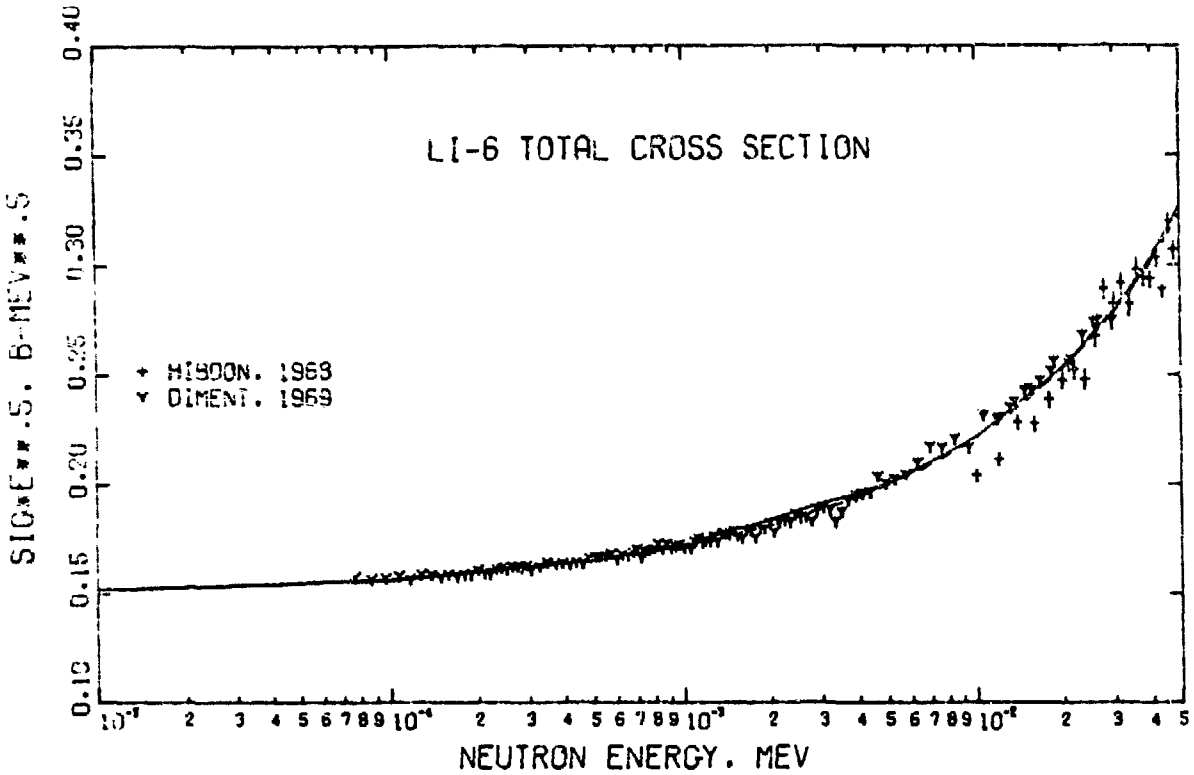

Fig. 11A.
The n-^{6}Li total cross section for E_n in the range 10 eV-50 keV. The data are from Refs. 74 and 83.

relationship among the cross sections near the $5/2^-$ resonance to allow the apparent discrepancy between the total and reaction cross sections to be resolved. Therefore, we cannot be confident that the (n,t) cross section resulting from this analysis represents the "true" cross section to standards accuracy over the resonance.

Recent work at Los Alamos is directed at resolving this perplexing question by supplementing direct measurements of the neutron cross sections with accurate

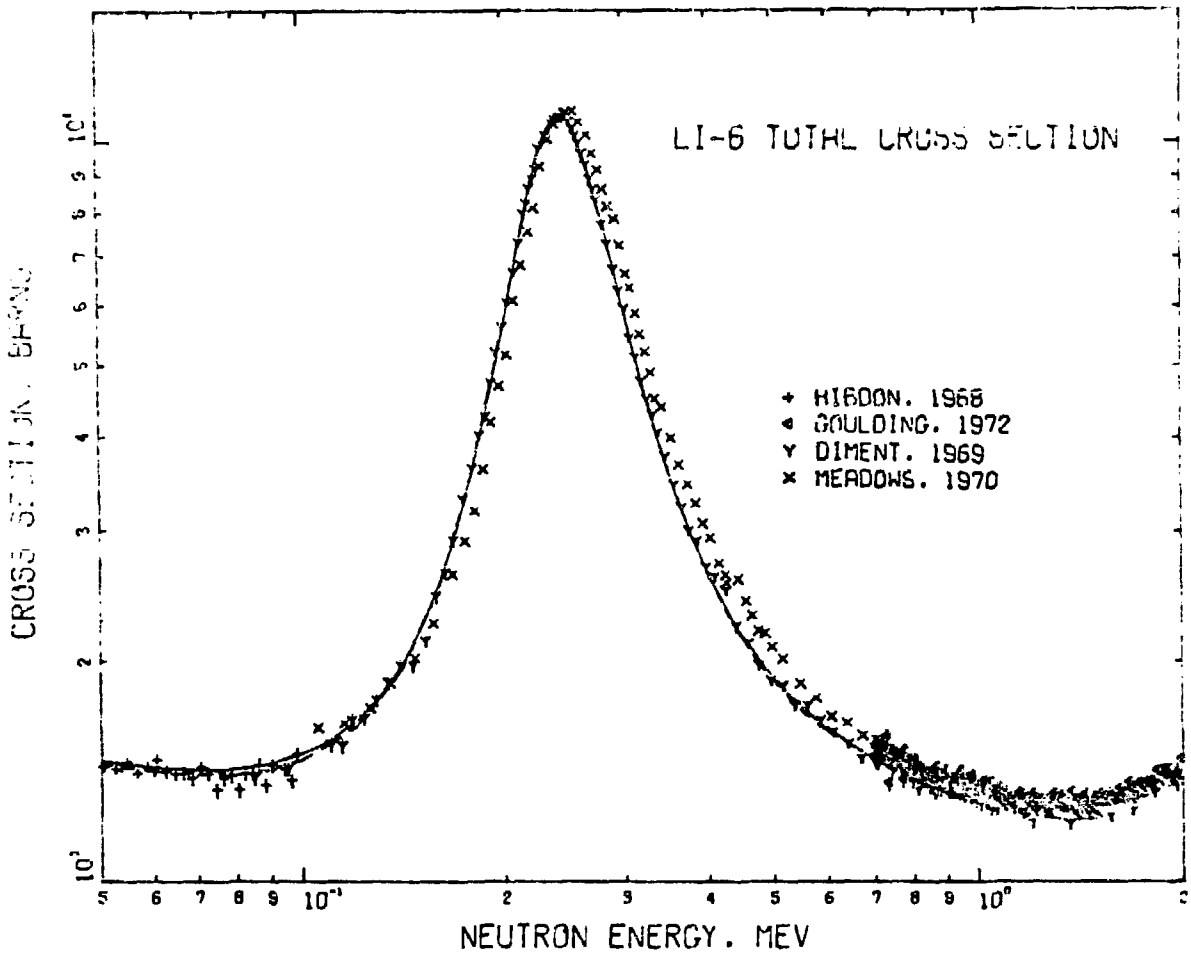

Fig. 11B.
The n-^{6}Li total cross section for E_n in the range 50 keV-2 MeV. The data are from Refs. 74, 75, 83, and 84.

charged-particle measurements for ^{4}He(t,t) scattering in the region of the resonance. Preliminary results which include this information were reported[86] at the Washington Nuclear Cross Sections and Technology Conference, and new results will be available for Version V of ENDF/B.

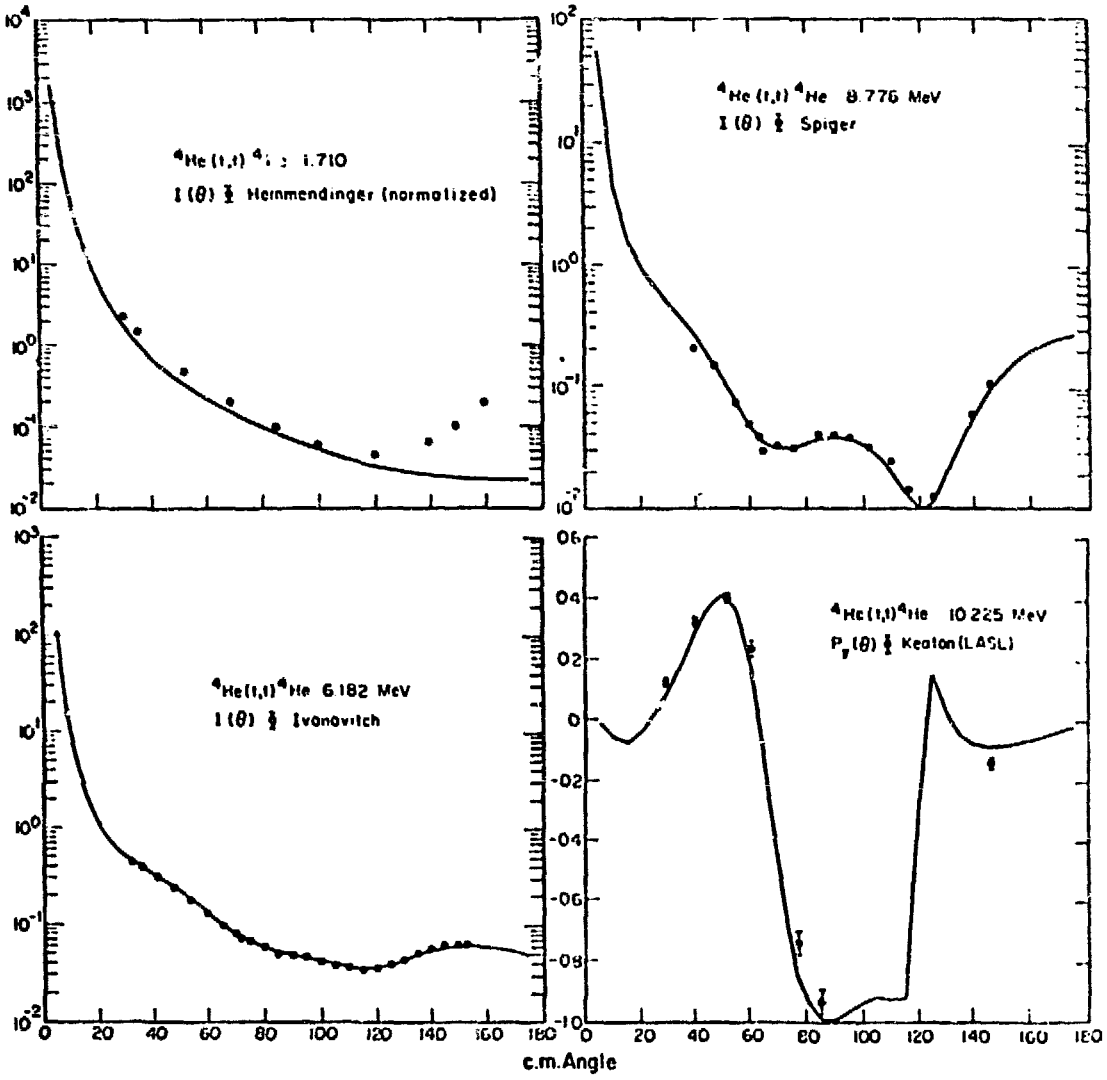

Fig. 12.

Representative fits to ^{4}He(t,t)^{4}He differential cross-section[76,77,85] and polarization[78] measurements for E_t in the range 1.7-10 MeV. The angular distribution at 8.776 MeV is close to the energy of the $5/2^-$ resonance at $E_n \approx 250$ keV. The units for I(θ) are b/sr.

V. $^{10}B(n,\alpha_0)^7Li$ AND $^{10}B(n,\alpha_1\gamma)^7Li^*$ CROSS SECTIONS

The $^{10}B(n,\alpha)$ cross section at low energies ($E_n < 1.0$ MeV) is based on a comprehensive R-matrix analysis of reactions in the ^{11}B system, similar to that described in the previous section for ^7Li. The two-body channel specifications used for this system are given in Table IV.

TABLE IV

CHANNEL QUANTITIES FOR THE ^{11}B SYSTEM ANALYSIS

Channel	Channel Radius (f)	Channel Spin (s)	ℓ_{max}
$n-^{10}B$	4.05	5/2, 7/2	1
$\alpha-^7Li(g.s)$	4.00	3/2	3
$\alpha-^7Li^*(0.478)$	6.17	1/2	3

Table V lists for each reaction the types of data considered, and references for the measurements included in the analysis.

TABLE V

DATA INCLUDED IN THE ^{11}B SYSTEM ANALYSIS

Reaction	Data Type	References
$^{10}B(n,n)^{10}B$	σ_{int}	87
	$\sigma(\theta)$, $P(\theta)$	87
$^{10}B(n,\alpha_0)^7Li$	σ_{int}	89, 90
	$\sigma(\theta)$	91
$^{10}B(n,\alpha_1)^7Li^*$	σ_{int}	92
$n-^{10}B$	σ_T	93
$^{10}B(n,\alpha_0+\alpha_1)$	σ_{int}	94
$^7Li(\alpha,\alpha)^7Li$	$\sigma(\theta)$ (E_α = 4-6 MeV)	95, 96
$^7Li(\alpha,\alpha')^7Li^*$	σ_{int} (E_α = 3-5 MeV)	97

Starting values for the resonance parameters were based on current information about the level scheme[87,95,98] of ^{11}B. The fits obtained from searching over the resonance parameters are discussed briefly by reaction in the sections below.

A. $^{10}B(n,n)^{10}B$

Two resonances are apparent in the elastic scattering data; a broad $7/2^+$ level which shows strongly in the integrated cross section at $E_n \approx 300$ keV, and a $5/2^-$ level which is evident in the differential cross-section and polarization data at 500 keV. Figure 13 shows that the fit to the integrated cross section reproduces the broad structure at 300 keV, and generally follows the data of Lane et al.[87] up to 1 MeV, although the calculated curve indicates a broader resonance than do Lane's data. Representative fits to the differential cross-section and polarization data are shown in Fig. 14. The change in the polarization from slightly negative at 375 keV to strongly positive at 850 keV indicates the presence of the $5/2^-$ level.

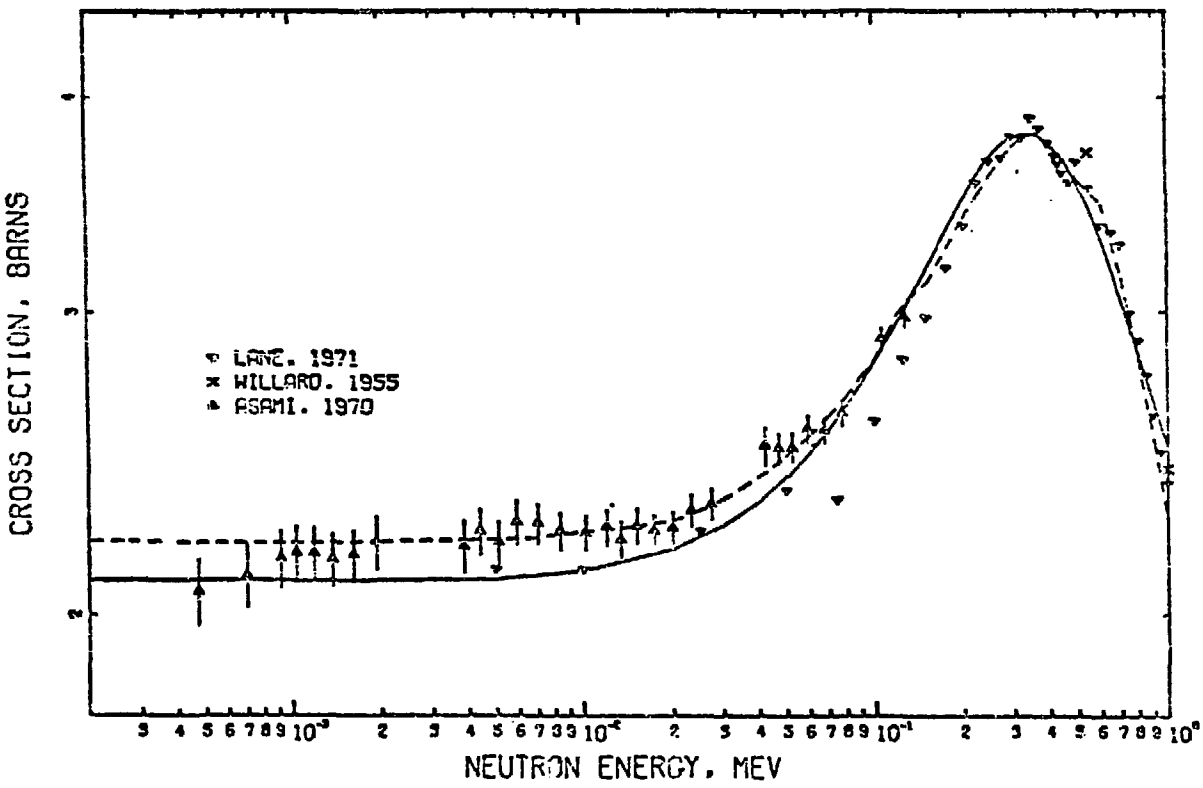

Fig. 13.
The $^{10}B(n,n)^{10}B$ integrated cross section for E_n between 0.2 keV and 1 MeV. The data are from Refs. 87, 88, and 99.

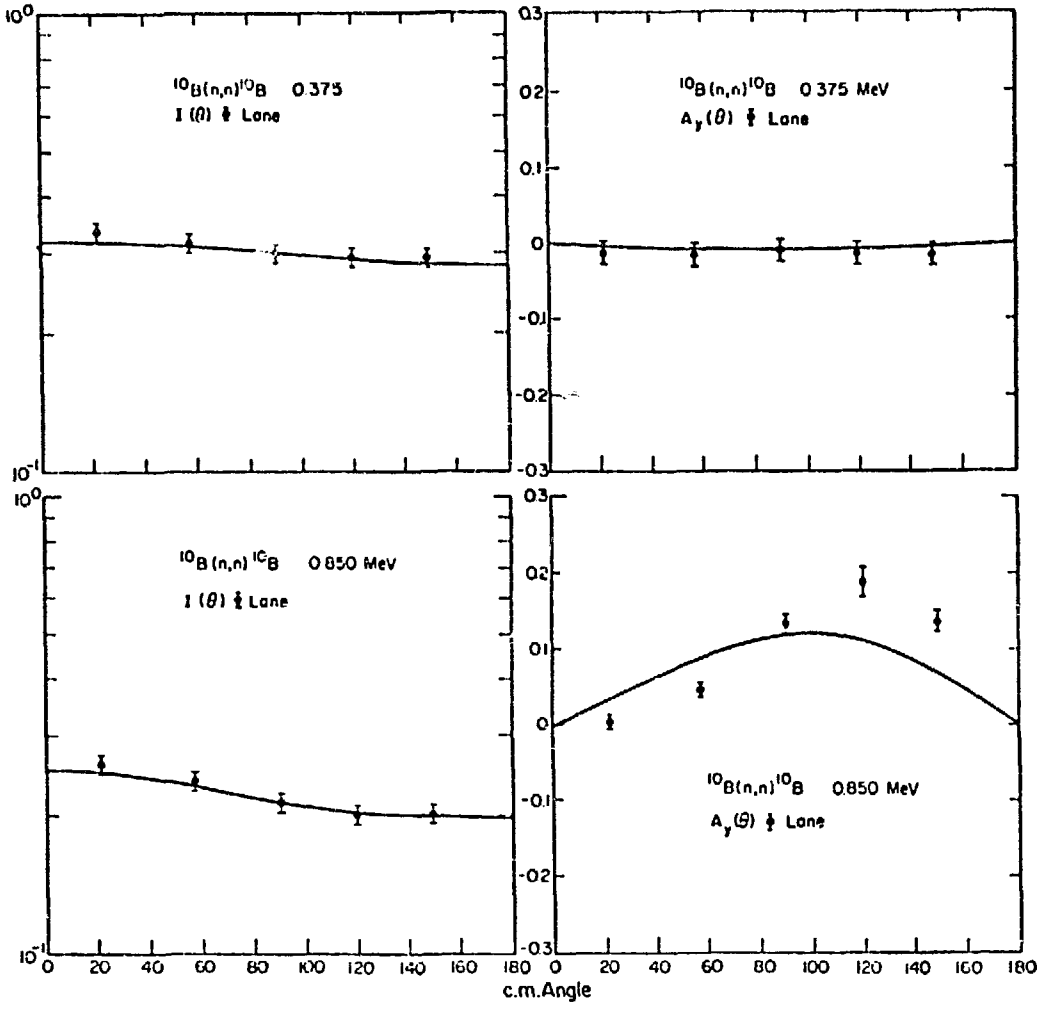

Fig. 14.
Representative fits to the $^{10}B(n,n)^{10}B$ differential cross section and polarization measurements of Lane[87] for E_n between 375 and 850 keV.

B. $^{10}B(n,\alpha_0)^7Li$ and $^{10}B(n,\alpha_1)^7Li^*$

The broad $7/2^+$ level evident in the elastic integrated cross section is largly responsible for the sizeable 1/v integrated cross section for these reactions. However, significant departures from the 1/v dependence occur above 100 keV, particularly in the (n,α_0) cross section. One of these deviations is due to the $5/2^-$ resonance discussed previously, and another is tentatively attributed to a $5/2^+$ level occurring at $E_n \approx 250$ keV. Figures 15A and 15B show the R-matrix fit to the separate (n,α_0) and (n,α_1) integrated cross sections. The upper curve follows the measurements of Macklin and Gibbons[89] quite closely

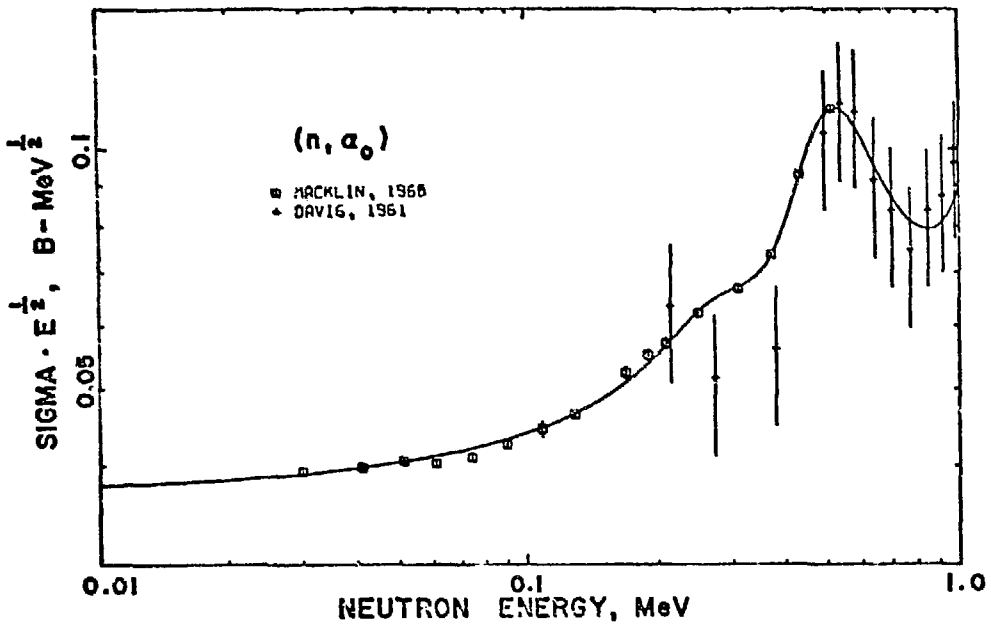

Fig. 15A.
The $^{10}B(n,\alpha_0)^7Li$ integrated cross section for E_n between 0.01 and 1 MeV. The data are from Refs. 89 and 90.

at the low energies, and those of Davis[90] above 500 keV. The lower curve agrees well with Friesenhahn's preliminary (n,α_1) data,[92] and follows the data of Davis above 500 keV. The calculated $^{10}B(n,\alpha_0+\alpha_1)$ cross section (Fig. 16) accurately reproduces the known thermal value of 3836.5 b., but does not pick up the detail of Mooring's measurements[94] in the 250-500 keV region. The fit to a selection of $^{10}B(n,\alpha_0)$ angular distributions measured by Van der Zwaan and Geiger[91] (actually for the inverse reaction) are shown in Fig. 17. The pronounced backward peaking of the angular distribution near 500 keV is due to the $5/2^-$ resonance.

C. $n-^{10}B$ σ_T

The calculated neutron total cross section is shown in Fig. 18 compared with various measurements. The agreement with Diment[93] is generally good, except at energies above 700 keV, where the calculated values approach more closely the measurements of Bockelman.[105]

D. $^7Li(\alpha,\alpha_0)^7Li$ and $^7Li(\alpha,\alpha_1)^7Li^*$

The $\alpha-^7Li$ reactions are considered in this analysis because they provide further unitary constraints on the neutron cross sections of interest, and because some of the resonances in this energy region show up prominently in these

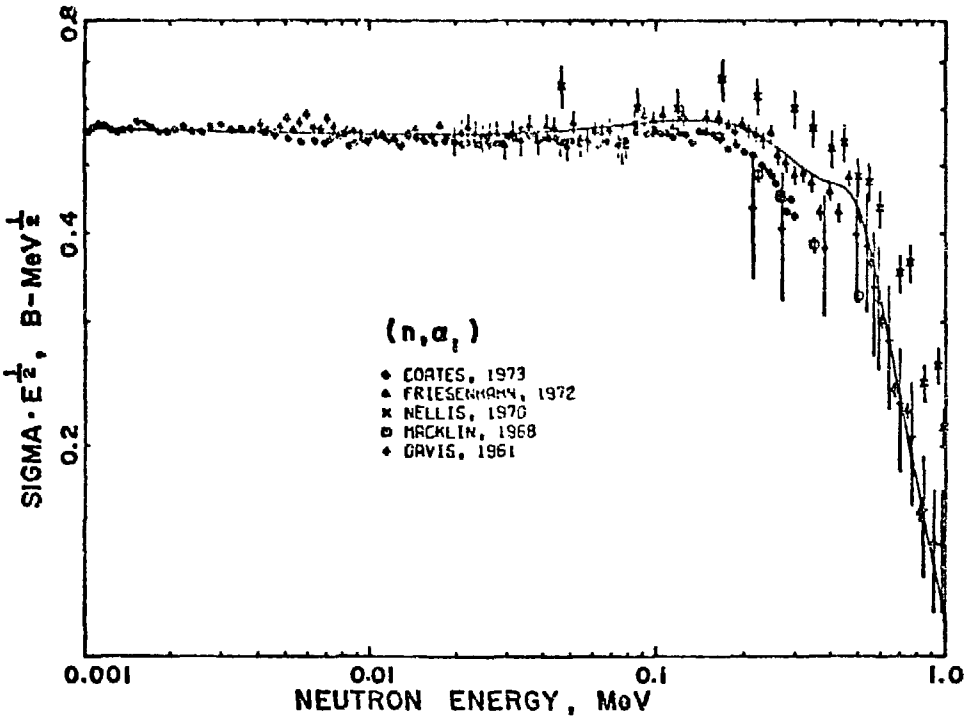

Fig. 15B.
The $^{10}B(n,\alpha_1)^7Li^*$ integrated cross section for E_n between 1 keV and 1 MeV. The data are from Refs. 71, 89, 90, 92, and 100.

reactions. Figure 19 shows fits to some of the $^7Li(\alpha,\alpha)^7Li$ angular distributions measured by Cusson.[95] Although these fits follow the qualitative features of the angular distributions, calculated values of the integrated (α_0,α_1) cross section indicate possible deficiencies in the level structure that are not apparent from considering the neutron reactions alone.

Evaluated neutron cross sections resulting from this R-matrix analysis at low energies agree well in most cases with the neutron data that were included in the analysis. However, $^{10}B(n,\alpha)$ data[82,106] that became available soon after the evaluation was submitted for ENDF/B-IV differ substantially from those used in the analysis. With sufficient data to determine the correct level structure, this comprehensive R-matrix approach can be expected to give a consistent set of smoothed cross sections that are determined more accurately than the individual measurements. In this case, we feel that present uncertainties in the data and in the level parameters limit the accuracy of the evaluated cross sections to

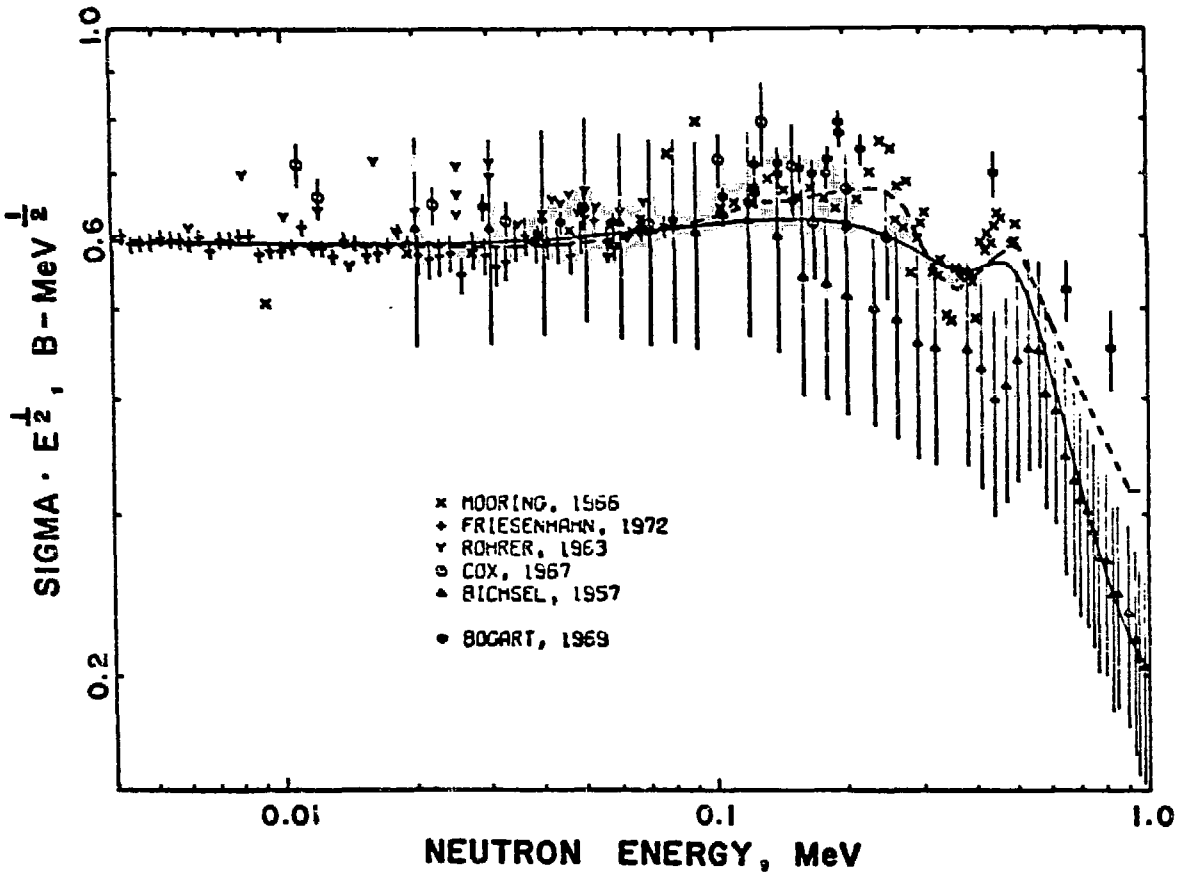

Fig. 16.
The summed $^{10}B(n,\alpha_0) + {}^{10}B(n,\alpha_1)$ integrated cross section for E_n between 4 keV and 1 MeV. The data are from Refs. 92, 94, 97, and 101-103.

~ 5% for $\sigma_{n,n}$ and σ_T, and as much as 20% for $\sigma_{n,\alpha}$ in the region between 200 keV and 1 MeV. The thermal value is probably determined to better than 1%, however, with the uncertainty in the evaluated (n,α) cross section increasing to ~ 5% at 200 keV.

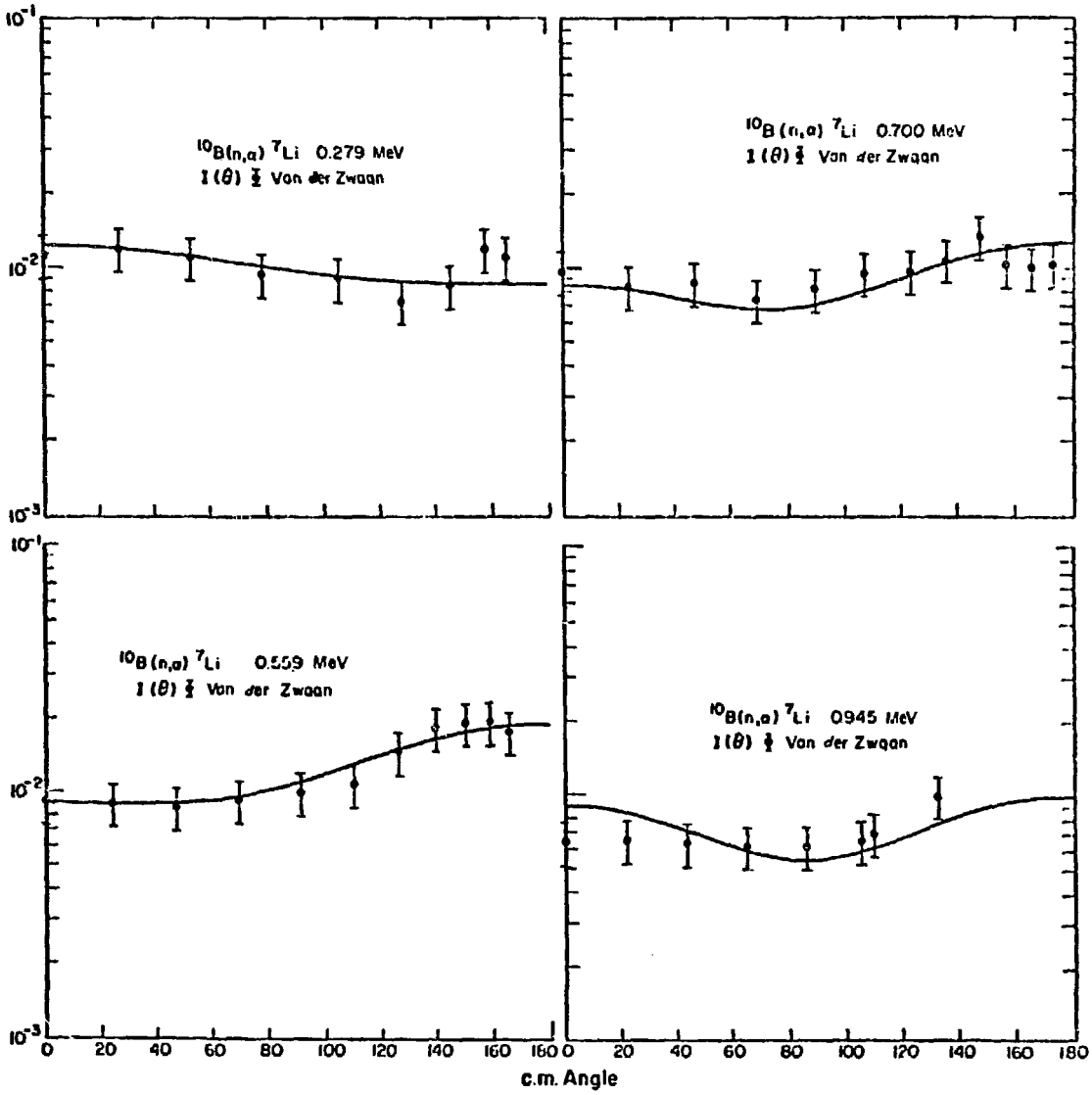

Fig. 17.
Representative fits to the $^{10}B(n,\alpha)^{7}Li$ differential cross-section measurements of Van der Zwaan and Geiger[91] for E_n between 279 and 945 keV. The units for I(θ) are b/sr.

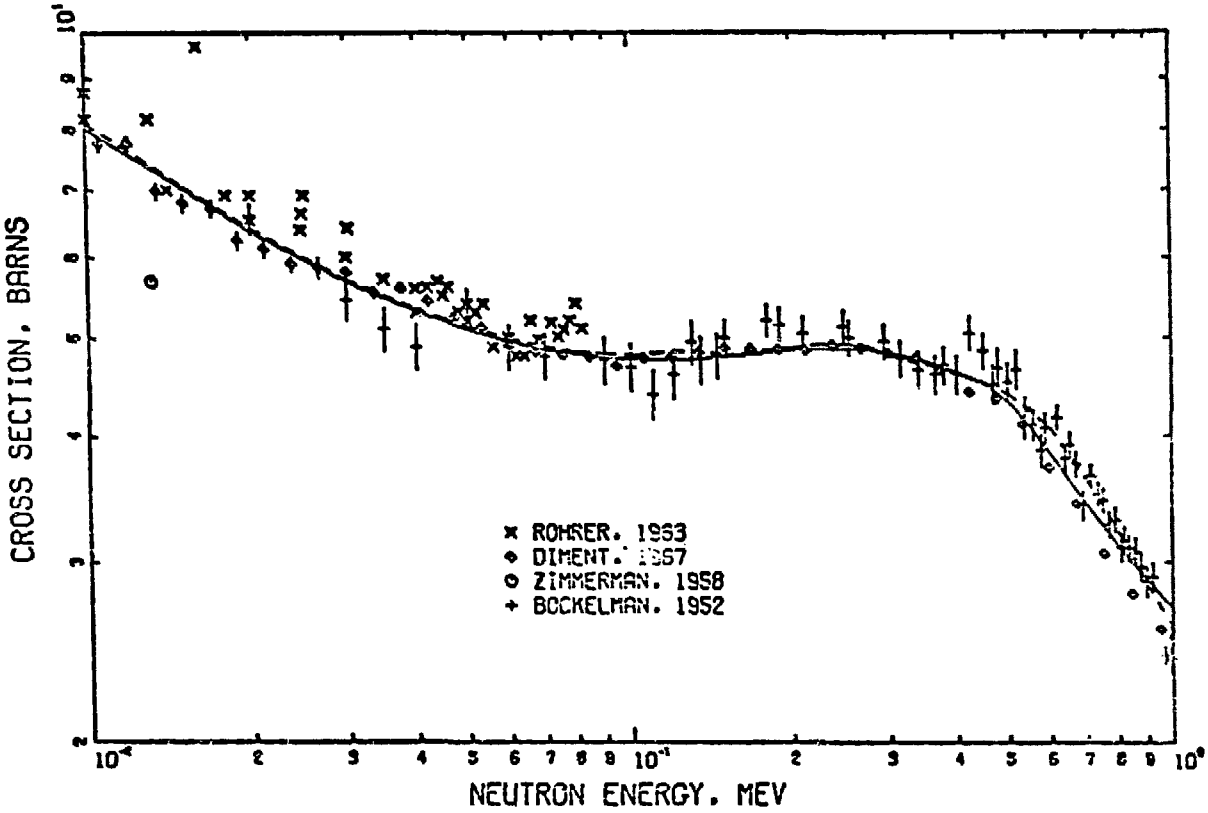

Fig. 18.
The n-^{10}B total cross section between 10 keV and 1 MeV. The data are from Refs. 93, 101, 104, and 105.

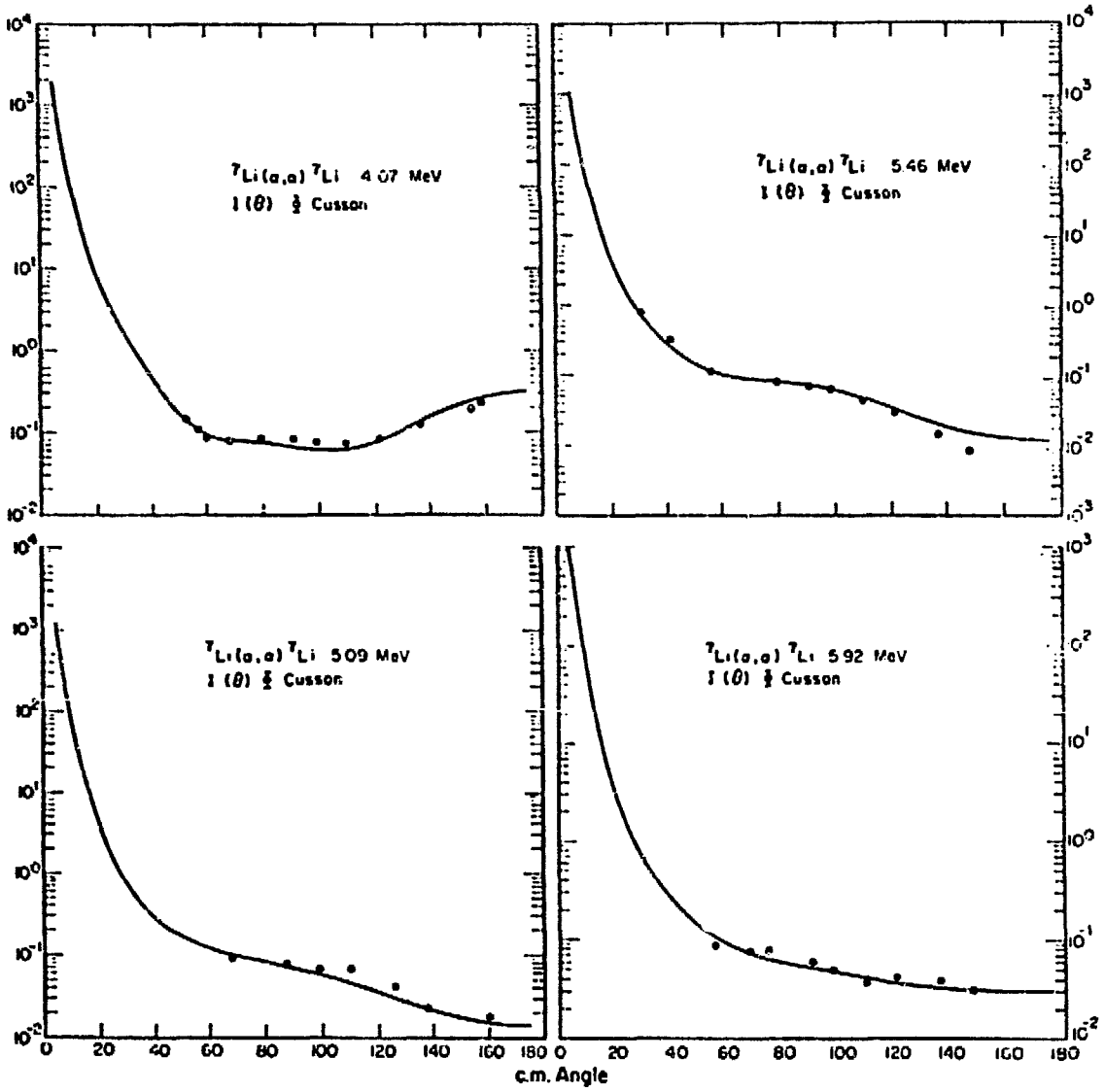

Fig. 19.
Representative fits to the ^{7}Li(α,α)^{7}Li differential cross-section measurements of Cusson[95] at alpha energies between 4 and 6 MeV. The units of I(θ) are b/sr.

REFERENCES

1. "ENDF/B Summary Documentation," ENDF-201, Compiled by D. Garber, (October 1975).

2. B. A. Magurno, Brookhaven National Laboratory Report, BNL-NCS-50464, ENDF-225 and INCD(US)-73/L (August 1975).

3. J. C. Hopkins and G. Breit, "The H(n,n)H Scattering Observables Required for High Precision Fast-Neutron Measurements," Nuclear Data A 9, 137 (1971) and private communication prior to publication (1970).

4. L. Stewart, R. J. LaBauve, and P. G. Young, "Evaluated Nuclear Data for Hydrogen in the ENDF/B-II Format," LA-4574 (1971). Neither the cross sections nor the angular distributions have been changed since Version II except to add one more significant figure to the total cross section.

5. R. E. Seamon, K. A. Friedman, G. Breit, R. D. Haracz, J. M. Holt, and A. Prakash, Phys. Rev. 165, 1579 (1968).

6. J. C. Hopkins, private communication to L. Stewart (1970).

7. J. C. Davis and H. H. Barschall, "Adjustments in the n-p Singlet Effective Range," Phys. Lett. 27B, 636 (1968).

8. E. Melkonian, "Slow Neutron Velocity Spectrometer Studies of O_2, N_2, A, H_2, H_2O, and Seven Hydrocarbons," Phys. Rev. 76, 1950 (1949).

9. D. H. Frisch, "The Total Cross Sections of Carbon and Hydrogen for Neutrons of Energies from 35 to 490 keV," Phys. Rev. 70, 589 (1946).

10. W. D. Allen and A. T. G. Ferguson, "The n-p Cross Section in the Range 60-550 keV," Proc. Phys. Soc. (London) 68, 1077 (1955).

11. E. Bretscher and E. B. Martin, "Determination of the Collision Cross-Section of H, Deuterium, C and O for Fast Neutrons," Helv. Phys. Acta 23, 15 (1950).

12. C. E. Engleke, R. E. Benenson, E. Melkonian, and J. M. Lebowitz, "Precision Measurements of the n-p Total Cross Section at 0.4926 and 3.205 MeV," Phys. Rev. 129, 324 (1963).

13. C. L. Bailey, W. E. Bennett, T. Bergstralh, R. G. Nuckolls, H. T. Richards, and J. H. Williams, "The Neutron-Proton and Neutron-Carbon Scattering Cross Sections for Fast Neutrons," Phys. Rev. 70, 583 (1946).

14. E. E. Lampi, G. Frier, and J. H. Williams, "Total Cross Section of Carbon and Hydrogen for Fast Neutrons," Phys. Rev. 76, 188 (1949).

15. W. E. Good and G. Scharff-Goldhaber, "Total Cross Sections for 900-keV Neutrons," Phys. Rev. 59, 917 (1941).

16. S. Bashkin, B. Petree, F. P. Mooring, and R. E. Peterson, "Dependence of Neutron Cross Sections on Mass Number," Phys. Rev. 77, 748 (1950).

17. R. E. Fields, R. L. Becker, and R. K. Adair, "Measurement of the Neutron-Proton Cross Section at 1.0 and 2.5 MeV," Phys. Rev. 94, 389 (1954).

18. C. L. Storrs and D. H. Frisch, "Scattering of 1.32 MeV Neutrons by Protons," Phys. Rev. 95, 1252 (1954).

19. D. G. Foster, Jr. and D. W. Glasgow, "Neutron Total Cross Sections, 2.5-15 MeV, Part 1 (Experimental)," Nucl. Instr. and Methods, 36, 1 (1967).

20. R. E. Fields, "The Total Neutron-Proton Scattering Cross Section at 2.5 MeV," Phys. Rev. 89, 908 (1953).

21. G. Ambrosina and A. Sorriaux, "Total Cross Section Efficiency for Carbon, Gluorine and Vanadium," Comptes Rendus 260, 3045 (1965).

22. W. H. Zinn, S. Seely, and V. W. Cohen, "Collision Cross Sections for D-D Neutrons," Phys. Rev. 56, 260 (1939).

23. N. Nereson and S. Darden, "Average Neutron Total Cross Sections in the 3- to 12- MeV Region," Phys. Rev. 94, 1678 (1954).

24. Y. Oda, J. Sanada, and S. Yamabe, "On the Angular Distribution of 3.1-MeV Neutrons Scattered by Protons," Phys. Rev. 80, 469 (1950).

25. E. M. Hafner, W. F. Hornyak, C. E. Falk, G. Snow, and T. Coor, "The Total n-p Scattering Cross Section at 4.75 MeV," Phys. Rev. 89, 204 (1953).

26. W. Sleator, Jr., "Collision Cross Sections of Carbon and Hydrogen for Fast Neutrons," Phys. Rev. 72, 207 (1947).

27. A. Bratenahl, J. M. Peterson, and J. P. Stoering, "Neutron Total Cross Sections in the 7- to 14-MeV Region," UCRL-4980 (1957).

28. A. H. Lasday, "Total Neutron Cross Sections of Several Nuclei at 14 MeV," Phys. Rev. 81, 139 (1951).

29. L. S. Goodman, "Total Cross Sections for 14-MeV Neutrons," Phys. Rev. 88, 686 (1952).

30. H. L. Poss, E. O. Salant, and L. C. L. Yuan, "Total Cross Sections of Carbon and Hydrogen for 14-MeV Neutrons," Phys. Rev. 85, 703 (1951).

31. M. Tanaka, N. Koori, and S. Shirato, "Differential Cross Sections for Neutron-Proton Scattering at 14.1 MeV," J. Phys. Soc. (Japan) 28, 11 (1970).

32. M. E. Battat, R. O. Bondelid, J. H. Coon, L. Cranberg, R. B. Day, F. Edeskuty, A. H. Frentrop, R. L. Henkel, R. L. Mills, R. A. Nobles, J. E. Perry, D. D. Phillips, T. R. Roberts, and S. G. Sydoriak, "Total Neutron Cross Sections of the Hydrogen and Helium Isotopes," Nucl. Phys. 12, 291 (1959).

33. J. C. Allred, A. H. Armstrong, and L. Rosen, "The Interaction of 14-MeV Neutrons with Protons and Deuterons," Phys. Rev. 91, 90 (1953).

34. C. F. Cook and T. W. Bonner, "Scattering of Fast Neutrons in Light Nuclei," Phys. Rev. 94, 651 (1954).

35. H. L. Poss, E. O. Salant, G. A. Snow, and L. C. L. Yuan, "Total Cross Sections for 14-MeV Neutrons," Phys. Rev. 87, 11 (1952).

36. P. H. Bowen, J. P. Scanlon, G. H. Stafford, and J. J. Thresher, "Neutron Total Cross Sections in the Energy Range 15 to 120 MeV," Nucl. Phys. 22, 640 (1961).

37. J. M. Peterson, A. Bratenahl, and J. P. Stoering, "Neutron Total Cross Sections in the 17- to 29-MeV Range," Phys. Rev. 120, 521 (1960).

38. D. E. Groce and B. D. Sowerby, "Neutron-Proton Total Cross Sections Near 20, 24, and 28 MeV," Nucl. Phys. 83, 199 (1966).

39. M. L. West II, C. M. Jones, and H. B. Willard, "Total Neutron Cross Sections of Hydrogen and Carbon in the 20-30 MeV Region," ORNL-3778, 94 (1965).

40. R. B. Day, R. L. Mills, J. E. Perry, Jr., and F. Schreb, "Total Cross Section for n-p Scattering at 20 MeV," Phys. Rev. 114, 209 (1959).

41. R. B. Day and R. L. Henkel, "Neutron Total Cross Sections at 20 MeV," Phys. Rev. 92, 358 (1953).

42. R. B. Schwartz, R. A. Schrack, and H. T. Heaton, "A Search for Structure in the n-p Scattering Cross Section," Phys. Lett. 30, 36 (1969).

43. J. M. Clement, P. Stoler, C. A. Goulding, and R. W. Fairchild, "Hydrogen and Deuterium Total Neutron Cross Sections in the MeV Region," Nucl. Phys. A 183, 51 (1972).

44. M. E. Remley, W. K. Jentschke, and P. G. Kruger, "Neutron-Proton Scattering Using Organic Crystal Scintillation Detectors," Phys. Rev. 89, 1194 (1953).

45. J. D. Seagrave, "Recoil Deuterons and Disintegration Protons from the n-d Interaction, and n-p Scattering at E_n = 14.1 MeV," Phys. Rev. 97, 757 (1955).

46. S. Shirato and K. Saitoh, "On The Differential Cross Section for Neutron-Proton Scattering at 14.1 MeV," J. Phys. Soc. (Japan) 36, 331 (1974).

47. T. Nakamura, "Angular Distribution of n-p Scattering at 14.1 MeV," J. Phys. Soc. (Japan) 15, 1359 (1960).

48. A. Suhami and R. Fox, "Neutron-Proton Small Angle Scattering at 14.1 MeV," Phys. Lett. 24, 173 (1967).

49. I. Basar, "Elastic Scattering of 14.4 MeV Neutrons on Hydrogen Isotopes," Few Body Problems Light Nuclei/Nucl. Interactions, Brela, 867 (1967).

50. F. Cambou, "Amelioratin des Methods de Spectrometrie des Neutrons Rapids," Thesis - U. of Paris, CEA-N-2002 (1961).

51. A. Galonsky and J. P. Judish, "Angular Distribution of n-p Scattering at 17.9 MeV," Phys. Rev. 100, 121 (1955).

52. This evaluation was translated by R. J. LaBauve into the ENDF/B format for Version III.

53. J. Als-Nielsen and O. Dietrich, "Slow Neutron Cross Sections for He^3, B, and Au," Phys. Rev. 133, B 925 (1964).

54. J. H. Gibbons and R. L. Macklin, "Total Neutron Yields from Light Elements under Proton and Alpha Bombardment," Phys. Rev. 114, 571 (1959).

55. R. L. Macklin and J. H. Gibbons, Proceedings of the International Conference on the Study of Nuclear Structure with Neutrons, Antwerp, 19-23 July 1965 (North-Holland Publishing Co., 1966), p. 498.

56. J. E. Perry, Jr., E. Haddad, R. L. Henkel, G. A. Jarvis, and R. K. Smith, private communication 1960.

57. R. Batchelor, R. Aves, and T. H. R. Skyrme, "Helium-3 Filled Proportional Counter for Neutron Spectroscopy," Rev. Sci. Instr. 26, 1037 (1955).

58. A. R. Sayres, K. W. Jones, and C. S. Wu, "Interaction of Neutrons with He^3," Phys. Rev. 122, 1853 (1961).

59. J. D. Seagrave, L. Cranberg, and J. E. Simmons, "Elastic Scattering of Fast Neutrons by Tritium and He^3," Phys. Rev. 119, 1981 (1960).

60. D. G. Costello, S. J. Friesenhahn, and W. M. Lopez, "$^3He(n,p)T$ Cross Section from 0.3 to 1.16 MeV," Nucl. Sci. Eng. 39, 409 (1970).

61. W. M. Lopez, M. P. Fricke, D. G. Costello, and S. J. Friesenhahn, "Neutron Capture Cross Sections of Tungsten and Rhenium," Gulf General Atomic, Inc. report GA-8835.

62. E. P. Wigner and L. Eisenbud, "Higher Angular Momenta and Long Range Interaction in Resonance Reactions," Phys. Rev. 72, 29 (1947).

63. D. C. Dodder, K. Witte, and G. M. Hale, "The LASL Energy-Dependent Analysis Code EDA," unpublished.

64. A. M. Lane and R. G. Thomas, "R-Matrix Theory of Nuclear Reactions," Rev. Mod. Phys. 30, 257 (1958).

65. L. Wolfenstein, "Polarization of Fast Neutrons," Ann. Rev. Nucl. Sci. 6, 43 (1956).

66. R. O. Lane, "Angular Distributions of Neutrons Scattered from Various Nuclei," Ann. Phys. 12, 135 (1961).

67. H. H. Knitter and A. M. Coppola, "Elastic Scattering of Neutrons from Li-6," EANDC (E)57(U) (1967).

68. H. B. Willard, J. K. Blair, J. D. Kington, and H. O. Cohn, "Elastic Scattering of Neutrons by Li-6 and Li-7," Phys. Rev. 101, 765 (1956).

69. R. O. Lane, A. J. Elwyn, and A. Langsdorf, Jr., "Polarization and Differential Cross Section for Neutrons Scattered from Li-6 and Li-7," Phys. Rev. 136, B 1710 (1964).

70. M. G. Sowerby, B. H. Patrick, C. A. Uttley, and K. M. Diment, "The Ratio of the ^{6}Li(n,α) and ^{10}B(n,α) Cross Sections from 10 eV to 80 keV and Recommended Values of the Cross Sections up to 200 keV," J. Nucl. Energy 24, 323 (1970).

71. M. S. Coates, G. J. Hunt, and C. A. Uttley, "Measurements of the Relative ^{6}Li(n,α) Cross Sections in the Energy Range 1 keV to 7500 keV," Neutron Standards Reference Data, IAEA, Vienna, p. 105 (1974).

72. W. P. Poenitz, "Measurements of the ^{6}Li(n,α)T Cross Section in the keV Energy Range," Z. Phys. 268, 359 (1974).

73. J. C. Overley, R. M. Sealock, and D. H. Ehlers, "^{6}Li(n,t)^{4}He Differential Cross Sections Between 0.1 and 1.8 MeV," Nucl. Phys. A 221, 573 (1974).

74. K. M. Diment and C. A. Uttley, "The Total Cross-Section of ^{6}Li," AERE-PR/NP 15, 12 (1969).

75. J. W. Meadows and J. F. Whalen, "The Total Neutron Cross Section of Lithium-6 from 100 to 1500 keV," Nucl. Sci. Eng. 48, 221 (1972).

76. M. Ivanovich, P. G. Young, and G. G. Ohlsen, "Elastic Scattering of Several Hydrogen and Helium Isotopes from Tritium," Nucl. Phys. A 110, 441 (1968).

77. R. J. Spiger and T. A. Tombrello, "Scattering of He^3 by He^4 by Tritium," Phys. Rev. 163, 964 (1970).

78. P. W. Keaton, Jr., D. D. Armstrong, and L. R. Vesser, "Polarization of Tritons Scattered from ^{4}He," Phys. Rev. Lett. 20, 1392 (1968).

79. F. Selove and T. Lauritsen, "Energy Levels of Light Nuclei A = 5-10," Nucl. Phys. A 227, 54 (1974).

80. A. Asami and M. C. Moxon, "Low Energy Neutron Scattering Cross Section of Li-6," 2nd IAEA Conference on Nuclear Data for Reactors, Helsinki, CN-26-25 (1970).

81. W. Fort and J. P. Marquette, "Experimental Methods Used at Cadarache to Determine the ^{6}Li(n,α)T Cross Section between 200 keV and 1700 keV," Proceedings of a Panel on Neutron Standard Reference Data, November 20-24 (1972), IAEA, Vienna.

82. S. J. Friesenhahn, V. J. Orphan, A. D. Carlson, M. P. Fricke, and W. M. Lopez, "(n,α) Cross Sections of ^{6}Li and ^{10}B between 1 and 1500 keV," Intelcom Rad Tech report INTEL-RT-7011-001 (Feb. 1974).

83. C. T. Hibdon, F. P. Mooring, "Total Neutron Cross Sections of ^{6}Li, ^{7}Li, and Li from 10 to 1236 keV," Conference on Neutron Cross Sections and Technology, Washington, D.C., Vol. I, 159 (1968).

84. C. A. Goulding and P. Stoler, "Total Neutron Cross Section of ^{4}He, ^{6}Li, and ^{7}Li from 0.5 to 30 MeV," EANDC(*S)-176U, p. 161 (1972).

85. A. Hemmendinger, "Cross Section for T-He^4 Scattering," Bull. Am. Phys. Soc. 1, 96 (1956).

86. G. M. Hale, "R-Matrix Analysis of the Light Element Standards," Proceedings of a Conference on Nuclear Cross Sections and Technology, Vol. I, 302 (1975).

87. R. O. Lane, A. S. Langsdorf, Jr., J. E. Monahan, and A. J. Elwyn, "Angular Distributions of Neutrons Scattered from Various Nuclei," ANL-6172 (1960).

88. A. Asami and M. C. Moxon, "Scattering Cross Sections of ^{10}B," AERE-PR/NP 14, 20 (1968).

89. R. L. Macklin and J. H. Gibbons, "Study of ^{10}B(n,α)^{7}Li, ^{7}Li* for [30 <E_n keV <500]," Phys. Rev. 165, 1147 (1968).

90. E. A. Davis, "The Disintegration of ^{10}B and ^{19}F by Fast Neutrons," Nucl. Phys. 27, 448 (1961).

91. L. Van der Zwaan and K. W. Geiger, "The ^{7}Li(α,n)^{10}B Differential Cross Section for Alpha Energies up to 8 MeV," Nucl. Phys. A 180, 615 (1972).

92. S. J. Friesenhahn, "Measurements of the ^{10}B(n,αγ) and ^{10}B(n,α) Cross Sections," Gulf-RT-A12210 (1972) (Preliminary).

93. K. M. Diment, "The Average Neutron Total Cross Section of ^{10}B from 100 eV to 10 MeV and Absorption Cross Section up to 500 keV," AERE-R-5224 (1967).

94. F. P. Mooring, J. E. Monahan, and C. M. Huddleston, "Neutron Cross Sections of the Boron Isotopes for Energies between 10 and 500 keV," Nucl. Phys. 82, 16 (1966).

95. R. Y. Cusson, "Levels in ^{11}B from ^{7}Li(α,α)^{7}Li and ^{7}Li(α,α1)^{7}Li* (0.48)," Nucl. Phys. 86, 481 (1966) and Thesis, California Institute of Technology (1965).

96. H. Bohlen, N. Marguardt, and W. Von Oertzen, "Nucleon Exchange in the Low-Energy Scattering of α-Particles on ^{6}Li and ^{7}Li," Nucl. Phys. A 179, 504 (1972).

97. H. Bischel and T. W. Bonner, "Reactions ^{7}Li(α,n)^{10}B, ^{7}Li(α,α')^{7}Li and ^{10}B(n,α)^{7}Li," Phys. Rev. 108, 1025 (1957).

98. F. Selove, "Energy Levels of Light Nuclei A = 11-12," Nucl. Phys. A 248, 6 (1975).

99. H. B. Willard, J. K. Bair, and J. D. Kington, "Elastic Scattering Angular Distributions of Fast Neutrons on Light Nuclei," Phys. Rev. 98, 669 (1955).

100. Donald O. Nellis, W. E. Tucker, and Ira L. Morgan, "Gamma-Ray Yield from Neutron Interactions with ^{10}B," Phys. Rev. C 1, 843 (1970).

101. R. H. Rohrer, private communication 1963 via the NNCSC.

102. S. A. Cox and F. R. Pontet, "Measurement of the $^{6}Li(n,absorption)$ and $^{10}B(n,absorption)$ Cross Sections by the Shell Transmission Method," J. Nucl. Energy 21, 271 (1967).

103. D. Bogart and L. L. Nichols, "Measurement of the $^{10}B(n,\alpha)^{7}Li$, $^{7}Li^{*}$ Relative Cross Sections in the keV Region," Nucl. Phys. 125, 463 (1969).

104. C. K. Bockelman, "Total Cross Sections of Be, B, O, and F for Fast Neutrons," Phys. Rev. 80, 1011 (1950).

105. R. L. Zimmerman, private communication (1958).

106. R. M. Sealock, "A Measurement of Differential Cross Sections for the $^{10}B(n,\alpha)^{7}Li$, $^{7}Li^{*}$ Reactions," Thesis, University of Oregon (1975).

☆ U.S. GOVERNMENT PRINTING OFFICE: 1976—777-018/9